



## Mesoscale modeling of combined aerosol and photo-oxidant processes in the eastern Mediterranean

M. Lazaridis, A. Spyridaki, S. Solberg, J. Smolík, V. ?dímal, K. Eleftheriadis,  
V. Aleksandropoulou, O. Hov, P. G. Georgopoulos

### ► To cite this version:

M. Lazaridis, A. Spyridaki, S. Solberg, J. Smolík, V. ?dímal, et al.. Mesoscale modeling of combined aerosol and photo-oxidant processes in the eastern Mediterranean. Atmospheric Chemistry and Physics Discussions, 2004, 4 (5), pp.5455-5514. hal-00301431

**HAL Id: hal-00301431**

**<https://hal.science/hal-00301431>**

Submitted on 21 Sep 2004

**HAL** is a multi-disciplinary open access archive for the deposit and dissemination of scientific research documents, whether they are published or not. The documents may come from teaching and research institutions in France or abroad, or from public or private research centers.

L'archive ouverte pluridisciplinaire **HAL**, est destinée au dépôt et à la diffusion de documents scientifiques de niveau recherche, publiés ou non, émanant des établissements d'enseignement et de recherche français ou étrangers, des laboratoires publics ou privés.

**Mesoscale modeling  
of combined aerosol  
and photo-oxidant  
processes**

M. Lazaridis et al.

# Mesoscale modeling of combined aerosol and photo-oxidant processes in the eastern Mediterranean

**M. Lazaridis<sup>1</sup>, A. Spyridaki<sup>1</sup>, S. Solberg<sup>2</sup>, J. Smolík<sup>3</sup>, V. Ždímal<sup>3</sup>,  
K. Eleftheriadis<sup>4</sup>, V. Aleksandropoulou<sup>1</sup>, O. Hov<sup>5</sup>, and P. G. Georgopoulos<sup>6</sup>**

<sup>1</sup>Technical University of Crete, Department of Environmental Engineering, 73100 Chania, Greece

<sup>2</sup>Norwegian Institute for Air Research (NILU), PO BOX 100, N 2007 Kjeller, Norway

<sup>3</sup>Institute of Chemical Process Fundamentals, ASCR, Prague, Czech Republic

<sup>4</sup>N.C.S.R. “Demokritos”, 15310 Agia Paraskevi, Athens, Greece

<sup>5</sup>Norwegian Meteorological Institute, PO Box 43 Blindern NO-0313 Oslo, Norway

<sup>6</sup>EOHSI, University of Medicine and Dentistry and Rutgers University, New Jersey, NJ, USA

Received: 11 June 2004 – Accepted: 29 June 2004 – Published: 21 September 2004

Correspondence to: M. Lazaridis (lazaridi@mred.tuc.gr)

Title Page

Abstract

Introduction

Conclusions

References

Tables

Figures

◀

▶

◀

▶

Back

Close

Full Screen / Esc

Print Version

Interactive Discussion

## Abstract

Particulate matter and photo-oxidant processes in the Eastern Mediterranean have been studied using the UAM-AERO mesoscale air quality model in conjunction with the NILU-CTM regional model. Meteorological data were obtained from the RAMS prognostic meteorological model. The modeling domain includes the eastern Mediterranean area between the Greek mainland and the island of Crete. The modeling system is applied to study the atmospheric processes in three periods, i.e. 13–16 July 2000, 26–30 July 2000 and 7–14 January 2001. The spatial and temporal distributions of both gaseous and particulate matter pollutants have been extensively studied together with the identification of major emission sources in the area. The modeling results were compared with field data obtained in the same period. Comparison of the modeling results with measured data was performed for a number of gaseous and aerosol species. The UAM-AERO model underestimates the PM<sub>10</sub> measured concentrations during summer but better comparison has been obtained for the winter data.

## 1. Introduction

Airborne particulate matter and photo-oxidants are important aspects of air pollution with very diverse effects ranging from human health to climate forcing. A major part of the aerosol mass is secondary particulate matter in the form of sulphate, nitrate, ammonium and organic aerosol particles formed by the oxidation of sulphur dioxide, nitrogen oxides and organic gaseous species. It is apparent that particulate matter is not a single pollutant and its mass includes a mixture of many pollutants distributed differently at different sizes.

Southern Europe is characterized with large changes over the past few decades linked to a large increase in population, and land-use alterations. The above changes had an impact on the atmospheric composition, water availability and consequently on quality of life, including potential impact on human health. For instance, most

## Mesoscale modeling of combined aerosol and photo-oxidant processes

M. Lazaridis et al.

Title Page

Abstract

Introduction

Conclusions

References

Tables

Figures

◀

▶

◀

▶

Back

Close

Full Screen / Esc

Print Version

Interactive Discussion

chemistry-transport models predict that the high ozone concentrations observed in summer over Europe are at a maximum around the Mediterranean sea, and more particularly in its Eastern part, exceeding very often the air quality standards and high concentrations of ozone and fine particles together were also observed (Lelieveld et al., 2002; Smolík et al., 2003). This is due to natural emissions of unsaturated hydrocarbons (including isoprene) which are highly reactive and continuing high emissions of anthropogenic gaseous and aerosol pollutants in Southern Europe (Hoffman et al., 1997; Pandis et al., 1992; Kavouras et al., 1998; Sotiropoulou et al., 2004). Aerosol yields obtained from experimental measurements and estimates (Pandis et al., 1992) also indicate that there are highly nonlinear aspects involved in the production of organic aerosols (e.g. the yields for the monoterpenes and peroxy radicals). In addition, human-induced forcing on the Mediterranean area is an increasing problem with complex consequences to quality of life and effects on radiative climate forcing.

It is therefore evident the need to study together the physico-chemical processes which control the dynamics of aerosols and photo-oxidants with a combination of modeling studies with extensive field measurements in the Mediterranean area. However, there is scarce information concerning consistent measurement/modelling studies combining regional, mesoscale and local scales to reveal the atmospheric composition/variability of particulate matter (PM)(Ackermann et al., 1998; Lurmann et al., 1997; Seigneur, 2001; Russell and Dennis, 2000; Pilinis and Seinfeld, 1987).

Based on the above facts two extensive measurement campaigns were performed to examine the characteristics and dynamics of photochemical pollutants and fine particles in the Eastern Mediterranean area between the Greek mainland and the island of Crete (Smolík et al., 2003). Sampling took place during 4 weeks in July 2000 and 1 week in January 2001 at the Finokalia station and onboard the research vessel Aigeaion. The Finokalia station (35°19' N, 25°40' E) is a remote coastal site eastward of Herakleion (the largest city of the island) atop a hill (elevation 130 m) facing the sea within the sector from 270° to 90° (Mihalopoulos et al., 1997).

Mihalopoulos et al. (1997) describe the Finokalia site in detail and report concen-

---

**Mesoscale modeling  
of combined aerosol  
and photo-oxidant  
processes**

M. Lazaridis et al.

---

[Title Page](#)[Abstract](#)[Introduction](#)[Conclusions](#)[References](#)[Tables](#)[Figures](#)[◀](#)[▶](#)[◀](#)[▶](#)[Back](#)[Close](#)[Full Screen / Esc](#)[Print Version](#)[Interactive Discussion](#)



trations of the major soluble ions collected over a one-year period. Ozone concentrations at Finokalia exhibit a well-defined seasonal cycle with a maximum during summer months and elevated levels (up to 80 ppbv) during daytime (summer) and over time periods of several days (summer) (Kouvarakis et al., 2000). Furthermore, ozone levels in the Eastern Mediterranean seem to be dominated by long range transport (Kouvarakis et al., 2000). In addition,  $\text{Nss-SO}_4$  and  $\text{SO}_2$  levels in Eastern Mediterranean were strongly influenced by regional transport (Sciare et al., 2003).

During the measurement campaigns an extensive range of instrumentation was employed to determine the physico-chemical characteristics of aerosol and gaseous pollutants. In particular, measurements focused on size-resolved sampling for the aerosol mass on a daily basis with subsequent analysis for ionic species, crustal and trace elements. In addition, total aerosol mass, equilibrium trace gasses, as well as detailed size-distribution measurements in terms of aerosol number by optical and differential mobility methods for the fine aerosol fraction were undertaken. Other complementary measurements included black carbon concentration by optical transmission methods, aerosol optical properties, and thermal analysis of selected samples. Relevant photo-oxidants and inorganic trace gases were monitored by prototype and conventional instruments.

Photochemical modeling is a necessary component in the study of the dynamics of gaseous pollutants and particulate matter since it provides the platform for the understanding of the variability and spatial-temporal patterns of these pollutants (Pilinis and Seinfeld, 1987; Binkowski and Shankar, 1995; Lurmann et al., 1997; Ackermann et al., 1998; Pai et al., 2000; Jacobson, 1997). A combined intensive modelling study and comparison with available experimental data for ozone/fine particles in the Mediterranean area should offer valuable information for characterizing their dynamics and association. The current modelling work covers short periods in summer and winter and the findings of this work have to be in perspective in relation with previous works in the same area of interest (Zerefos et al., 2002; Bardouki et al., 2003; Sciare et al., 2003; Kouvarakis et al., 2000).

---

## Mesoscale modeling of combined aerosol and photo-oxidant processes

M. Lazaridis et al.

---

[Title Page](#)[Abstract](#)[Introduction](#)[Conclusions](#)[References](#)[Tables](#)[Figures](#)[◀](#)[▶](#)[◀](#)[▶](#)[Back](#)[Close](#)[Full Screen / Esc](#)[Print Version](#)[Interactive Discussion](#)

The specific objective of the current modeling work is mainly to evaluate and assess the importance of the local sources versus the transport component for the ambient concentration of the photochemical pollutants and fine particles in the eastern Mediterranean area. Another objective is the importance of the natural sources for the concentration of the particulate matter and ozone. The comparison between experimental field data and modeling results is aiming to verify the model applicability in the area under study and show the general physico-chemical characteristics of ambient gaseous and aerosol components.

A detailed modeling study has been performed using the UAM-AERO mesoscale air quality model (Lurmann et al., 1997). Meteorological input data were provided by the RAMS (Pielke et al., 1992) prognostic meteorological model whereas gaseous regional data on background concentrations were obtained from the NILU-CTM model (Flatøy et al., 2000) and on particulate matter from the EMEP model (Simpson et al., 1995). The present study represents one of the first applications of a modified UAM-AERO model combined with the prognostic meteorological model (RAMS) for the southern Mediterranean and comparison between modeled and measured data for particulate matter. In addition, the current modeling application is one of the first ones to study combined aerosol and photo-oxidant processes together with extensive comparisons with field data.

Predicted aerosol and gaseous species concentrations patterns in the eastern Mediterranean area show the importance of the long range transport component and the significance of the natural emission sources. In agreement with previous studies (Lurmann et al., 1997) it is observed that the model performance is sensitive to a number of parameters but mainly to particulate matter emission characteristics. Determination of the aerosol wind resuspension is an important factor to evaluate the importance of the crustal material contribution in to the aerosol mass size distribution. Poor agreement for specific particulate matter chemical components mainly during the summer period reflects the uncertainty in the emission inventory data.

---

**Mesoscale modeling  
of combined aerosol  
and photo-oxidant  
processes**

---

M. Lazaridis et al.

---

[Title Page](#)[Abstract](#)[Introduction](#)[Conclusions](#)[References](#)[Tables](#)[Figures](#)[◀](#)[▶](#)[◀](#)[▶](#)[Back](#)[Close](#)[Full Screen / Esc](#)[Print Version](#)[Interactive Discussion](#)

## 2. Material and methods

### 2.1. Description of the domain

The model domain (58×74 grid points), covers SE Greece (the inner black rectangular included in Fig. 1). Five vertical layers were used: two below and three above the diffusion break. The grid was defined in the UTM coordinate system. The UTM zone 34 was used for the definition of the grid above Greece, which means a central meridian of 21° E. The SW corner coordinates of the grid are the following (according to the WGS84 system) Easting: 692089 and Northing: 3868229. This corresponds to the geographical coordinates: 34°56′08″ latitude and 23°06′02″ longitude.

The region of interest includes marine (the Aegean and Cretan Seas), islanded (Cyclades, Crete) and continental (Attica and Peloponnesus) parts of southern Greece. A complicated topography (high mountains, deep sea and small islands scattered all over the sea), combined with the prolonged sunny and humid periods, the strong winds and the presence of one of the most polluted European cities (Athens) on the NW, inhabited by almost half of the country's population, comprise the quite interesting character of the area.

On the southern part of the modeling domain is the island of Crete which is located at the south of Greece, mid-distance between Athens and the northern African coast. It is mainly mountainous, with all major cities located at the north coast. The total population rises up to 600 000, while at summer periods this number can increase significantly, due to a high load of tourism, part of which is scattered all over the island, but the majority is mainly concentrated along the northern coast.

The modelling results are compared with extensive measurements performed at the Finokalia which is a remote coastal site, situated on the top of a hill (elevation 130 m), at the NE part of the island (Smolík et al., 2003). In addition, the modelling results were compared with measurements performed on board a research vessel during July 2000 and with limited data in the city of Herakleion on Crete, 70 km west from the Finokalia site.

## Mesoscale modeling of combined aerosol and photo-oxidant processes

M. Lazaridis et al.

Title Page

Abstract

Introduction

Conclusions

References

Tables

Figures

◀

▶

◀

▶

Back

Close

Full Screen / Esc

Print Version

Interactive Discussion

The emissions inputs, except for PM<sub>10</sub> which were obtained from TNO (Berdowski et al., 1998), are from the EMEP database, from the CTM-NILU regional model (initial and background concentrations) and from detailed emission inventories for biogenic species (isoprene and terpenes), resuspended dust and sea salt (Alexandropoulou and Lazaridis, 2004; Lazaridis et al., 2003). The background and initial concentrations for the 24 gaseous species considered in the model were obtained from the CTM-NILU regional model (Flatøy et al., 2000).

In detail among atmospheric pollutants, CO, SO<sub>x</sub>, NO<sub>x</sub>, NMVOC, NH<sub>3</sub> and PM were selected for the study and their spatial resolution was increased using the allocation of emissions in several sources (EMEP/CORINAIR, 2002), landuse and population density data. Particular interest was given in the estimation of natural emissions and especially for NMVOC (isoprene, terpene) emitted by vegetation, sea salt particles and resuspended soil dust (Andreae, 1995; Alexandropoulou and Lazaridis, 2004).

Emission estimates were compiled using the methodology given in “Atmospheric Emissions Inventory Guidebook”, CORINAIR (EMEP/CORINAIR, 2002). A bottom-up approach is followed in the evaluation of biogenic and natural emissions using landuse and meteorology data (Simpson et al., 1995, 1999). Hourly temporal resolution is used for the natural emissions whereas the anthropogenic data were evaluated as annual averages. Furthermore, the emissions were spatially allocated on a 5×5 km<sup>2</sup> grid.

An example of the surface ozone and nitrogen oxides surface background concentrations calculated with the CTM-NILU model is presented in Fig. 1, where high ozone and NO<sub>x</sub> concentrations are calculated downwind of the Athens metropolitan area. The above initial concentrations, representing 3-D hourly values (in ppm) were also used as background concentrations of the domain.

## 2.2. The three-dimensional photochemical modeling and prognostic meteorological tools

The UAM-AERO mesoscale model is a gas/aerosol air quality model that is based on the model UAM version IV (Lurmann et al., 1997). Several modifications have

### Mesoscale modeling of combined aerosol and photo-oxidant processes

M. Lazaridis et al.

Title Page

Abstract

Introduction

Conclusions

References

Tables

Figures

◀

▶

◀

▶

Back

Close

Full Screen / Esc

Print Version

Interactive Discussion

been introduced in the UAM-AERO mesoscale model, including new preprocessors for biogenic and natural emissions. The emission inventories are based on EMEP data (EMEP, 2003), whereas more detailed inputs for biogenic emissions, resuspended dust, sodium and chlorine were calculated using newly developed methodologies combined with the UAM-AERO model. Simulations were initiated 24 h before the beginning of each modeling period for having minimum effect on the model results from the initial conditions.

The UAM-AERO allows the use of various alternative chemical mechanisms. The one employed for this case study is the Carbon Bond-IV (CB-IV), where species are lumped according to the type of their C-C bonds. A large number of reactions, involving 47 species are taken into account.

The meteorological inputs were obtained using the RAMS (version 4.29) prognostic meteorological model (Pielke et al., 1992). RAMS combines a non-hydrostatic cloud model (Tripoli and Cotton, 1982) and a hydrostatic mesoscale model (Mahrer and Pielke, 1977). It was developed for simulating atmospheric phenomena with resolutions ranging from tens of kilometers to a few meters. There is no lower limit to the domain size or to the mesh cell size of the model finite difference grid. A general description of the model and its capabilities is given in Pielke et al. (1992).

### 2.3. Application of the modeling system in the eastern Mediterranean

The combined UAM-AERO and RAMS modelling framework has been applied to model the summer and winter campaigns of the SUB-AERO programme which performed in two sites: the Finokalia station on the island of Crete (Greece) and aboard the research vessel "Aigeaion", which cruised across the Eastern Mediterranean area between the Greek mainland and the island of Crete. Sampling took place during 4 weeks in July 2000 and at Finokalia for 1 week in January 2001.

The simulations have been conducted for two distinguished periods (July 2000, January 2001), in an attempt to investigate on the seasonal differences in the fate of the pollutants. Two sub-periods have been examined for the summer period: 13–16 and

## Mesoscale modeling of combined aerosol and photo-oxidant processes

M. Lazaridis et al.

Title Page

Abstract

Introduction

Conclusions

References

Tables

Figures

◀

▶

◀

▶

Back

Close

Full Screen / Esc

Print Version

Interactive Discussion

26–30 of July, the second one chosen to coincide with the marine part of the campaign. The interest is focused on the understanding of the tropospheric gaseous and aerosol background of the area in question. At the same time, a comparison between summer and winter model results is attempted.

Extensive simulations have been performed during July 2000 and January 2001. The synoptic conditions over the Central and Eastern Mediterranean in July 2000 were characterized by a high-pressure system over the Central and Eastern Mediterranean and Northern Africa. The passage of relatively shallow disturbances over Southern Europe towards the Balkans and the Black Sea resulted in the strengthening of the pressure gradient over NW Turkey and the Dardanelles Gap. As a result, a westerly flow was evident on 15 and 16 while on the following seven days the Etesians were established. Between 18–28 July 2000 the air masses reached Finokalia from the north. They originated mainly from the western coast of the Black Sea and during the last three days of this period, where peak mass concentrations were observed, from the Aegean Sea. On the last two days, trajectories originated from north of Crete, moved first to Africa and then changed direction, finally arriving at the Finokalia site from the southeast.

During the winter period the meteorological conditions were characterised by a low pressure system which on 6 January lay over the eastern part of the Mediterranean. A relatively strong northerly flow was evident over the NE Mediterranean, which dissipated throughout the following 24 h as the depression drew away towards the Middle East. To the west, a deep and extended Atlantic depression covered Central and Southern Europe. This system reached the Central Mediterranean on 8 January and then moved north-eastward through the Balkans towards the Black Sea. From 8 to 9 January a southerly synoptic flow was established over the area of interest. As the depression moved away towards the Black Sea, a high-pressure system progressively developed over the Central Mediterranean. On 10 January a relatively strong north-westerly synoptic flow was apparent over the Central and NE part of the Mediterranean. This flow dissipated throughout the following 24 h. On 11 to 12 January, the synoptic

Mesoscale modeling  
of combined aerosol  
and photo-oxidant  
processes

M. Lazaridis et al.

Title Page

Abstract

Introduction

Conclusions

References

Tables

Figures

◀

▶

◀

▶

Back

Close

Full Screen / Esc

Print Version

Interactive Discussion

flow over the area under consideration was relatively weak. The wind field over the land was modified by the landscape. Over the Aegean maritime area a weak northerly current was established while over the Central Mediterranean and the Ionian Sea the synoptic flow was westerly. On 13 January a new depression from the west reached the Central Mediterranean while a strong anticyclonic circulation dominated over Central and Eastern Europe. These synoptic conditions favoured the development of a strong pressure gradient over the NE Mediterranean region. A strong southerly flow was evident over the Ionian Sea and the southern part of the Aegean while a strong easterly-north-easterly flow prevailed to the north.

The predicted spatial distribution of the concentration of ozone, nitrogen dioxide, sulphur dioxide, sodium, ammonium in aerosol phase, carbon monoxide, resuspended dust and total  $PM_{10}$  are presented in Fig. 2 for 30 July 2000. Their spatial distribution reveals higher concentrations of particulate matter, carbon monoxide, nitrogen dioxide and ozone downwind the Athens metropolitan area and also highlights the importance of the transport of pollutants from outside the modelling domain. This regional transport is related with the prevailing meteorological conditions. The predicted pattern of  $O_3$  shows a band of high concentrations extending from the Athens metropolitan area to the middle of the Aegean Sea and lower concentrations in a narrow area at the western part of the domain and above the island of Crete.

The concentration of aerosol and gaseous pollutants in the area under study is dependent on the prevailing meteorological conditions and anthropogenic emissions due to regional transport infiltrate in few hours to the centre of the domain as shown in Fig. 2 for  $O_3$ ,  $NO_2$ ,  $SO_2$ , PM and CO. Natural emissions such as sea salt and resuspended dust are correlated with the meteorological fields in the modelling domain. The spatial distribution of  $PM_{10}$  encounters the production of sea salt and agrees well with the primary PM emission patterns. The spatial pattern of sodium is high over the Aegean sea and at lower levels onshore, which decreases at higher distances from the coastline. The spatial patterns agree well with the primary PM emission patterns.

A daily variation of the  $PM_{10}$  concentration is shown in Fig. 3. The Fig. 3 depicts

**Mesoscale modeling  
of combined aerosol  
and photo-oxidant  
processes**

M. Lazaridis et al.

Title Page

Abstract

Introduction

Conclusions

References

Tables

Figures

◀

▶

◀

▶

Back

Close

Full Screen / Esc

Print Version

Interactive Discussion



the dynamic change in the concentration of pollutants in the eastern Mediterranean due to meteorological changes and emissions from local areas. In the morning of 14 July strong northwestern winds transport particulate matter from the Athens area to the southern part of the Aegean Sea and also result in considerable sea salt emissions.

5 The same meteorological conditions prevail until 10:00 h. At this time then the wind changes to north as depicted in Fig. 3b. From 17:00 h there is a decrease on the wind velocity and we have more stagnant meteorological conditions and finally at 21:00 h west wind directions are more pronounced. It is evident that the meteorological conditions are responsible to a large extent for the dynamics of the pollutant concentrations  
10 in the area and the consequent human exposure. Elevated particulate matter concentrations are expected both with air-mass origins from the west/north-west (western Europe and continental Greece) and the south. The former would carry anthropogenic produced aerosols (with size distributions mainly in the fine sector), while the latter contribute to increases of coarse PM, transporting dust from North Africa and the Saharan desert. The Black Sea is expected also to contribute in anthropogenic aerosols (combustion, etc.), as well, while easterlies can contribute both to fine and coarse modes, depending on whether the air-parcel crosses urban or desert areas.

The regional transport for ozone and particulate matter can be also depicted in Fig. 4 where we present the surface concentration for the period 13–16 July 2000 at 12:00 h.  
20 A north westerly flow during this period is shown in Fig. 4 where elevated concentrations of ozone and particulate matter infiltrate in the modelling domain. The same behaviour is also depicted for several chemical components such as carbon monoxide, nitrogen oxides, sulphur dioxide and volatile organic components.

Regional transport in the Mediterranean area of ozone and other pollutants is also occurring at higher altitudes and at the free troposphere as studied in several previous works (Kouvarakis et al., 2000; Lelieveld et al., 2002). In the present modelling study regional transport of ozone, particulate matter and other gaseous pollutants contributes to the pollutant levels at the area under study. An average vertical profile for the ozone concentration during the January 2001 is shown in Fig. 5 for three different environ-  
25

---

**Mesoscale modeling  
of combined aerosol  
and photo-oxidant  
processes**M. Lazaridis et al.

---

[Title Page](#)[Abstract](#)[Introduction](#)[Conclusions](#)[References](#)[Tables](#)[Figures](#)[◀](#)[▶](#)[◀](#)[▶](#)[Back](#)[Close](#)[Full Screen / Esc](#)[Print Version](#)[Interactive Discussion](#)



ments, one at Finokalia where the measurements were occurred, one above an urban area (Herakleion) and the other an average profile above the marine area. Ozone values range between 29 and 36 ppb, for the whole winter modelling period. The ozone exhibits a daily profile, depending in a great extent to the mixing height fluctuations.

5 Infiltration of ozone from the free troposphere to the surface area contributes to enhanced concentration levels. However, there are scarce data on the vertical profiles of pollutants in the area and no comparison with the modelling results can be performed.

The importance of the regional transport of  $PM_{10}$  and  $O_3$  in the area of interest has been further examined using the UAM-AERO model and setting the particulate emissions in the modelling domain to zero. The average reduction in the  $PM_{10}$  concentration in the modelling domain ranged from 60% to 45% for the summer and winter modelling periods respectively. It is evident from these results the importance of the regional transport to the  $PM_{10}$  concentration in the eastern Mediterranean area. These results reflect the prevailing meteorological conditions which occurred during the modelling period and are not including forest fire emissions and the Saharan dust input. Since the modelling period corresponds to a few days no certain conclusions can be drawn for longer periods. However, the current results support previous studies in the area which showed the importance of the long range transport of pollutants in the Mediterranean area (Sciare et al., 2003; Zerefos et al., 2002).

20 Comparison with the experimental field data during summer and winter periods are shown in Fig. 6 for  $O_3$ . The measurements were performed at the northern part of the island of Crete, at the Finokalia station, at the town of Herakleion (Crete, 70 km west from Finokalia) and onboard the research vessel Aigeaion. As can be seen, the variation of the modeled results follows the same characteristics as the measured data during the measured period. Also, the diurnal variation of the predicted concentrations has been found to be in qualitative agreement with the measured data.

25 Figure 7 shows the average modelled daily profile of the speciated  $PM_{10}$ , for the period between 13 and 16, 26 and 30 July 2000 and finally between 7–14 January 2001. The dominating species is the crustal material due to the resuspension from the soil

---

**Mesoscale modeling  
of combined aerosol  
and photo-oxidant  
processes**M. Lazaridis et al.

---

[Title Page](#)[Abstract](#)[Introduction](#)[Conclusions](#)[References](#)[Tables](#)[Figures](#)[◀](#)[▶](#)[◀](#)[▶](#)[Back](#)[Close](#)[Full Screen / Esc](#)[Print Version](#)[Interactive Discussion](#)

surface at the summer period. Elemental carbon is expected to be underestimated, mainly due to the large number of fires in Greece at this period, a factor not taken into account by the model. Other important species are ammonium, sulphur, nitrates and of course sea-salt particles. From the speciated PM<sub>10</sub> mass data it is important to note the significance of the natural contribution (crustal oxides, sodium, chlorine) to the particulate matter mass during the summer period (close to 54%). During the winter period the natural contribution is smaller (close to 31%). However, it has to be noted that the modelling period covers only a very small time interval and not certain conclusions can be drawn for longer periods. Figure 7c presents the average PM<sub>10</sub> concentration during the winter campaign for the site of Finokalia (January 2001). The dominating species are sulfates, nitrates, and crustal material. Other important compounds are Na<sup>+</sup> and Cl<sup>-</sup>, mainly due to the fact that Finokalia is a coastal site.

In Tables 1–2 we present average predicted and observed concentrations for chemical resolved particulate matter species during the summer and winter simulation periods. The comparison for the particulate matter is concentrated on the 24-h average predictions. The comparison for the total PM<sub>10</sub> mass is better in the winter period compared to the summer. Ammonium sulfate and crustal materials dominate the PM<sub>10</sub> mass whereas nitrate and sea salt are also important species in the chemical mass closure.

Tables 3–5 contain the field concentration of trace gases, including those in equilibrium with aerosol species and their comparison with the modeling results for the Finokalia station during the summer period, at the research vessel Aigeaion and at Finokalia during the winter period. The modeling data follow the same trends as the experimental field results.

Figure 8 shows a comparison between calculated and measured daily average PM<sub>10</sub> levels for both the summer and winter periods. There is a considerable underestimation for the PM<sub>10</sub> mass during summer and a more acceptable trend in the winter. At 12, 27 and 28 July Saharan dust episodes were identified to contribute significantly to the ambient PM<sub>10</sub> concentration. This is the reason for the significant discrepancies between

---

**Mesoscale modeling  
of combined aerosol  
and photo-oxidant  
processes**

M. Lazaridis et al.

---

[Title Page](#)[Abstract](#)[Introduction](#)[Conclusions](#)[References](#)[Tables](#)[Figures](#)[◀](#)[▶](#)[◀](#)[▶](#)[Back](#)[Close](#)[Full Screen / Esc](#)[Print Version](#)[Interactive Discussion](#)

modeled and measured data. The average  $\text{PM}_{10}$  value from the modeling studies over the whole winter simulation period is  $9.3 \mu\text{g}/\text{m}^3$  whereas for the summer period the value is  $21.1 \mu\text{g}/\text{m}^3$ . The corresponding value for the measured data reaches the  $14.6 \mu\text{g}/\text{m}^3$  for the winter period and  $33.5 \mu\text{g}/\text{m}^3$  for the summer period. The difference in the concentration levels can be also attributed to the underestimation of a number of chemical components present in the particulate mass. For example there is an underestimation of Chlorine and Sodium (sea-salt) particulate matter emissions, as well as, underestimation of the sulphate mass and crustal materials from Saharan dust episodes. In addition, forest fires in July 2000 contributed to PM mass but they were not included in the modelling study. Furthermore, an important fraction of the measured particulate matter has not been chemically identified and this corresponds to the overall uncertainty in the comparison between model results and measured data. However, the  $\text{SO}_4^{2-}$ ,  $\text{NO}_3^-$ ,  $\text{NH}_4^+$ , OC and EC concentrations are generally in good agreement with the measured data as shown in Tables 1–2.

Figure 9 presents a comparison between measured and predicted  $\text{SO}_4^{2-}$  levels, for the site of Finokalia during the second measurement campaign in January 2001. The agreement between modeling and measurement data is satisfactory. Sources of  $\text{SO}_4^{2-}$  are considered to be mainly anthropogenic from the Greek mainland and from long range transport. Co-variation with gaseous  $\text{SO}_2$  and  $\text{H}_2\text{SO}_4$  proves the anthropogenic origin from gas precursors. The  $\text{SO}_4^{2-}$  particles are mainly emitted from industrial sources. The existence of the State Electricity Organization power plant at the city of Herakleion, as well as air-masses that originate from Athens can strongly influence the levels observed at the island of Crete.

Figure 10 shows the comparison between modeled and measured concentrations for  $\text{Na}^+$ . Particles that originate from the sea are strongly affected by the wind and the contribution to the Finokalia station which is a coastal station is very important. The modeling data in general are in good agreement with the measured data except on 11 January where the measured average  $\text{Na}^+$  concentration is close to  $0.5 \mu\text{g}/\text{m}^3$  whereas the modeling value is  $1.7 \mu\text{g}/\text{m}^3$ .

## Mesoscale modeling of combined aerosol and photo-oxidant processes

M. Lazaridis et al.

Title Page

Abstract

Introduction

Conclusions

References

Tables

Figures

◀

▶

◀

▶

Back

Close

Full Screen / Esc

Print Version

Interactive Discussion

Despite the fact that the simulation periods are short to enable extraction of seasonal trends of pollutants, differences between summer and winter periods are clear both at quantitative and diurnal variation patterns observed. Pollutants strongly dependent on solar activity exhibit a more stable throughout the day pattern. At the same time the values measured at winter are a lot lower than the ones corresponding to the summer period for the cases of ozone, isoprene, PAN, OH and other photooxidants, while the levels of their precursors appear elevated ( $\text{NO}$ ,  $\text{NO}_2$ , etc.). Especially, particulate matter concentrations are lower during winter mainly due to reduced dust resuspension from the soil and small photochemical activity.

From the modeling results and the comparison with the measured data it can be resulted that the Eastern Mediterranean is characterized by a quite heavy aerosol load during summer from anthropogenic ( $\text{SO}_4^{2-}$ ,  $\text{NO}_3^-$ ), biogenic ( $\text{NH}_4^+$ ), Saharan dust and sea-emitted/natural ( $\text{Na}^+$ ,  $\text{Cl}^-$ ) aerosols. Transport contributes significantly on the high levels observed at remote sites. Most common species are related to the existence of sulfate, nitrate, ammonium ions, sea salt and Saharan dust, with the formation of  $(\text{NH}_4)_2\text{SO}_4$  to be of the most important secondary aerosol as also observed from measurements and supported from the modeling results (Kouvarakis et al., 2002).

### 3. Conclusions

The combined UAM-AERO/RAMS modeling system is an efficient platform for simulating the transport/dynamics of particulate matter and photo-oxidant precursors. The UAM-AERO model has been applied to simulate the dynamics of PM and photo-oxidants in the eastern Mediterranean area.

The modeling studies with the combined UAM-AERO and CTM-NILU reveal the importance of photo-oxidant and fine aerosols dynamics in the Mediterranean area and the significant contribution of regional transport in the observed pollution levels. Meteorological data were obtained from the RAMS system. Comparison of the modelling results with measured data leads to an underestimation of the  $\text{PM}_{10}$  measured con-

## Mesoscale modeling of combined aerosol and photo-oxidant processes

M. Lazaridis et al.

Title Page

Abstract

Introduction

Conclusions

References

Tables

Figures

◀

▶

◀

▶

Back

Close

Full Screen / Esc

Print Version

Interactive Discussion

centrations during summer. During the winter experimental campaign the comparison between the model results and the experimental data is better.

Discrepancies between modelled and measured data for the particulate matter are mainly due to unresolved particulate matter emissions such as Saharan dust and forest fire emissions. The measured values show that resuspension from soil is an important factor in determining the aerosol size distribution during the summer period. This fact demonstrates the need for chemical quantification of particulate matter emission inventories in Europe, as well as the need for better determination of the effect of Saharan dust, wild forest fires, and resuspended dust emissions in Southern Europe.

The particulate matter is mainly composed by sulfate, sea salt and crustal materials with also significant amounts of nitrate, ammonium and organics. In general the area of the eastern Mediterranean is moderately to highly polluted during summer with a contribution from the main urban conglomerations, whereas during the winter period the particulate matter and oxidant concentrations are lower than the summer values.

*Acknowledgements.* This work was supported by the European Commission under grant ENVK2-1999-00052. We also would like to thank S. Pandis (Carnegie Mellon University) for his helpful comments and suggestions.

## References

- Ackermann, I. J., Hass, H., Memmesheimer, M., Ebel, A., Binkowski, F. S., and Shankar, U.: Modal aerosol dynamics model for Europe: Development and first applications, *Atmos. Environ.*, 32, 2981–2999, 1998.
- Aleksandropoulou, V. and Lazaridis, M.: Study of gaseous and particulate matter emissions in Greece, *Water Air and Soil Pollution*, 153, 15–34, 2004.
- Andreae, M. O.: In *Future Climates of the World: A Modelling perspective* (Climatic effects of changing atmospheric aerosol levels), edited by Henderson-Sellers, A., Macquarie University, Climatic Impacts Centre, Australia, 1995.
- Bardouki, H., Liakakou, H., Economou, C., Sciare, J., Smolík, J., Ždímal, V., Eleftheriadis, K., Lazaridis, M., and Mihalopoulos, N.: Chemical composition of size resolved atmospheric

## Mesoscale modeling of combined aerosol and photo-oxidant processes

M. Lazaridis et al.

Title Page

Abstract

Introduction

Conclusions

References

Tables

Figures

◀

▶

◀

▶

Back

Close

Full Screen / Esc

Print Version

Interactive Discussion

aerosols in the eastern Mediterranean during summer and winter, Atmos. Environ., 37, 195–208, 2003.

Benkovitz, C. M., Scholtz, M. T., Pacyna, J., Tarrason, L., Dignon, J., Voldner, E. C., Spiro, P. A., Logan, J. A., and Graedel, T. E.: Global gridded inventories of anthropogenic emissions of sulfur and nitrogen, J. Geophys. Res.-A., 101, (D22), 29 239–29 253, 1996.

Berdowski, J. J. M., Mulder, W., Veldt, C., Visschedijk, A. J. H., and Zandveld, P. Y. J.: Particulate matter emissions (PM<sub>10</sub>-PM<sub>2.5</sub>-PM<sub>0.1</sub>) in Europe in 1990 and 1993, Technical Report, Netherlands organization for Applied Scientific Research, TNO-MEP-R 96/472, Apeldoorn, The Netherlands, 1997.

Binkowski, F. S. and Shankar, U.: The regional particulate model, 1. Model description and preliminary results, J. Geophys. Res., 100, 26 191–26 209, 1995.

EMEP/CORINAIR: 'Atmospheric Emission Inventory Guidebook', 3rd Edition, Prepared by the EMEP Task force on Emission Inventories, EEA Technical Report No. 30, 2002.

EMEP-WMO: Workshop on Strategies for Monitoring of Regional Air Pollution in relation to the need within EMEP, GAW and other international bodies, EMEP/CCC-Report 10/97, 1997.

Flatøy, F., Hov Ø., and Schlanger, H.: Chemical forecasts used for measurement flight planning during the POLINAT 2, Geophys. Res. Lett., 27, 951–954, 2000.

Guenther, B., Zimmerman, P. R., Harley, P. C., Monson, R. K., and Fall, R.: Isoprene and monoterpene rate variability: Model evaluations and sensitivity analysis, J. Geophys. Res., 10, 12 609–12 617, 1993.

Jacobson, M. Z.: Development and application of a new air pollution modeling system – II: Aerosol module structure and design, Atmos. Environ., 31A, 131–144, 1997.

Kallos, G., Kotroni, V., Lagouvardos, K., and Papadopoulos, A.: On the transport of air pollutants from Europe to North Africa, Geophys. Res. Lett., 25, 5, 619–622, 1999.

Kouvarakis, G., Tsigaridis, K., Kanakidou, M., and Mihalopoulos, N.: Temporal variations of surface regional background ozone over Crete Island in the southeast Mediterranean, J. Geophys. Res., 105, 4399–4407, 2000.

Lazaridis, M., Spiridaki, A., Solberg, S., Kallos, G., Svendby, T., Flatoy, F., Drossinos, I., Housiadas, C., Smolik, J., Colbeck, I., Varinou, M., Gofa, F., Eleftheriadis, K., Zdimal, V., and Georgopoulos, P. G.: Modelling of combined aerosol and photooxidant processes in the Mediterranean area, Water Air and Soil Pollution – Focus, in press, 2004.

Lelieveld, J., Berresheim, H., Borrmann, S., Crutzen, P. J., Dentener, F. J., Fischer, H., Fehichter, J., Flatau, P. J., Heland, J., Holzinger, R., Korrmann, R., Lawrence, M. G., Levin, Z.,

## Mesoscale modeling of combined aerosol and photo-oxidant processes

M. Lazaridis et al.

Title Page

Abstract

Introduction

Conclusions

References

Tables

Figures

◀

▶

◀

▶

Back

Close

Full Screen / Esc

Print Version

Interactive Discussion

- Markowicz, K. M., Mihalopoulos, N., Minikin, A., Ramanathan, V., de Reus, M., Roelofs, G. J., Scheeren, H. A., Sciare, J., Schlager, H., Schultz, M., Siegmund, P., Steil, B., Stephanou, E. G., Stier, P., Traub, M., Warneke, C., Williams, J., and Ziereis, H.: Global air pollution crossroads over the Mediterranean, *Science*, 298, 794–799, 2002.
- 5 Lurmann, F. W., Wexler, A. S., Pandis, S. N., Mussara, S., Kumar, N., and Seinfeld, J. H.: Modelling Urban and Regional Aerosols – II. Application to California's South Coast Air Basin, *Atmos. Environ.*, 31, 2695–2715, 1997.
- Mihalopoulos, N., Stephanou, E., Kanakidou, M., Pilitsidis, S., and Bousquet, P.: Tropospheric aerosol ionic composition in the Eastern Mediterranean region, *Tellus Ser. B-Chem. Phys. Meteorol.*, 49, 314–326, 1997.
- 10 Monahan, E. C., Spiel, D. E., and Davidson, K. L.: A model of marine aerosol generation via whitecaps and wave disruption, in *Oceanic whitecaps*, edited by Monahan, E. C. and Mac Niocail, G., 167–174, D. Reidel, Norwell, MA, 1986.
- Pai, P., Vijayaraghavan, K., and Seigneur, C.: Particulate matter modeling in the Los Angeles basin using the SAQM-AERO, *J. Air & Waste Management Association*, 50, 32–42, 2000.
- 15 Pandis, S. N., Harley, R. A., Cass, G. R., and Seinfeld, J. H.: Secondary organic aerosol formation and transport, *Atmos. Environ.*, 26A, 2269–2282, 1992.
- Peters, L. K., Berkowitz, C. M., Carmichael, G. R., Easter, R. L., Fairweather, G., Ghan, S. J., Hales, J. M., Leung, L. R., Pennell, W. R., Potra, F. A., Saylor, R. D., and Tsang, T. T.: The current state and future direction of eulerian models in simulating tropospheric chemistry and transport of trace species: a review, *Atmos. Environ.*, 29, 189–222, 1995.
- 20 Pielke, R. A., Cotton, W. R., Walko, R. L., Tremback, C. J., Lyons, W. A., Grasso, L. D., Nicholls, M. E., Moran, M. D., Wesley, D. A., Lee, T. J., and Copeland, J. H.: A comprehensive Meteorological Modeling System – RAMS, *Meteorol. Atmos. Phys.*, 49, 69–91, 1992.
- 25 Pilinis, C. and Seinfeld, J. H.: Continued development of a general equilibrium model for inorganic multicomponent atmospheric aerosols, *Atmos. Environ.*, 21, 2453–2466, 1987.
- Russell, A. and Dennis, R.: NARSTO critical review of photochemical models and modeling, *Atmos. Environ.*, 34, 2283–2324, 2000.
- Sciare, J., Bardouki, H., Moulin, C., and Mihalopoulos, N.: Aerosol sources and their contribution to the chemical composition of aerosols in the Eastern Mediterranean Sea during summertime, *Atmos. Chem. Phys.*, 3, 291–302, 2003.
- 30 Seigneur, C.: Current status of air quality models for particulate matter. *Journal of the Air and the Waste Management Association*, 51, 1508–1521, 2001.

## Mesoscale modeling of combined aerosol and photo-oxidant processes

M. Lazaridis et al.

Title Page

Abstract

Introduction

Conclusions

References

Tables

Figures

◀

▶

◀

▶

Back

Close

Full Screen / Esc

Print Version

Interactive Discussion

- Seinfeld, J. H. and Pandis, S. N.: Atmospheric chemistry and physics, From air pollution to Climate change, John Wiley and Sons Inc., New York, 1998.
- Simpson, D., Guenther, A., Hewitt, C. N., and Steinbrecher, R.: Biogenic emissions in Europe, J. Geophys. Res., 100, D11, 22 875–22 890, 1995.
- 5 Simpson, D., Winiwarter, W., Borjesson, G., et al.: Inventorying emissions from nature in Europe, J. Geophys. Res. 104, D7, 8113–8152, 1999.
- Smith, M. H., Park, P. M., and Consterdine, I. E.: Marine aerosol concentration and estimated fluxes over seas, Q. J. R. Meteorol. Soc., 809–824, 1993.
- Smolík, J., Ždímal, V., Schwarz, J., Lazaridis, M., Havránek, V., Eleftheriadis, K., Mihalopoulos, N., Bryant, C., and Colbeck, I.: Size resolved mass concentration and elemental composition of atmospheric aerosols over the Eastern Mediterranean area, Atmos. Chem. Phys., 3, 2207–2216, 2003.
- 10 Sotiropoulou, R. E. P., Tagaris, E., Pilinis, C., Andronopoulos, S., Sfetsos, A., and Bartzis, J. G.: The BOND project: Biogenic aerosols and air quality in Athens and Marseille greater areas, J. Geophys. Res., 109, D05205, 2004.
- Thomas, G. E. and Stamnes, K.: Radiative Transfer in the Atmosphere and Ocean, Cambridge University Press, New York, 1999.
- Zerefos, C. S., Kourtidis, K., Melas, D., Balis, D., Zanis, P., Katsaros, L., Mantis, H. T., Repapis, C., Isaksen, I., Sundet, J., Herman, J., Bhartia, P. K., and Calpini, B.: Photochemical Activity and Solar Ultraviolet Radiation (PAUR) Modulation Factors: An overview of the project, J. Geophys. Res., D18, 8134–8148, 2002.
- 20

## Mesoscale modeling of combined aerosol and photo-oxidant processes

M. Lazaridis et al.

Title Page

Abstract

Introduction

Conclusions

References

Tables

Figures

◀

▶

◀

▶

Back

Close

Full Screen / Esc

Print Version

Interactive Discussion



**Mesoscale modeling  
of combined aerosol  
and photo-oxidant  
processes**

M. Lazaridis et al.

**Table 1.** Comparison between experimental field data and modelling results (particulate matter chemical components) for the July 2000 period at the Finokalia station.

$\mu\text{g}/\text{m}^3$	Model Results	Experimental (Arith. Mean)
	July 2000 (Average)	July 2000 (Average)
Total PM10	20.8	33.54
SO <sub>4</sub> =1	5.04	6.30
NO <sub>3</sub> -1	2.23	2.48
NH <sub>4</sub> +1	1.58	2.20
Na+1	1.72	1.92
Cl-1	1.28	1.99
EC	0.17	0.44*
OC	1.04	1.32*
Crustal Oxides <sup>#</sup>	8.13	7.58 <sup>#</sup>

Title Page

Abstract

Introduction

Conclusions

References

Tables

Figures

◀

▶

◀

▶

Back

Close

Full Screen / Esc

Print Version

Interactive Discussion

**Mesoscale modeling  
of combined aerosol  
and photo-oxidant  
processes**

M. Lazaridis et al.

Title Page

Abstract

Introduction

Conclusions

References

Tables

Figures

◀

▶

◀

▶

Back

Close

Full Screen / Esc

Print Version

Interactive Discussion

**Table 2.** Comparison between experimental field data and modelling results (particulate matter chemical components) for the January 2001 period at the Finokalia station.

$\mu\text{g}/\text{m}^3$	Model Results	Experimental (Arith. Mean)
	January 2001 (Average)	January 2001 (Average)
Total PM10	9.35	14.55
SO <sub>4</sub> =1	2.18	2.14
NO <sub>3</sub> –1	2.50	1.46
NH <sub>4</sub> +1	0.77	0.79
Na+1	1.11	1.11
Cl–1	0.59	1.88
EC	0.20	0.15*
OC	0.83	0.45*
Crustal Oxides <sup>#</sup>	1.14	1.37 <sup>#</sup>

\* TSP

<sup>#</sup>  $1.16 \cdot (1.90 \cdot \text{Al} + 2.15 \cdot \text{Si} + 1.41 \cdot \text{Ca} + 1.67 \cdot \text{Ti} + 2.09 \cdot \text{Fe})$

**Mesoscale modeling  
of combined aerosol  
and photo-oxidant  
processes**

M. Lazaridis et al.

**Table 3.** Comparison between experimental field data and modelling results (gaseous species) for the July 2000 period at the Finokalia station.

Parameter	Finokalia (Summer) (ppbv)	Model Results (ppbv)
O <sub>3</sub>	60	50
NO <sub>2</sub>	2.25*** (10–20/7)	1
NO	<0.05	0.03
SO <sub>2</sub>	0.84 *	0.6
HNO <sub>3</sub>	0.45* (20–30/7)	0.1
	0.15** (10–20/7)	
HONO	0.13** (10–20/7)	0.05

\* from annular denuder measurements

\*\* prototype wet effluent diffusion denuder technique/chemiluniscnt detection

\*\*\* prototype chemiluminescence ozone and nitrogen dioxide detectors

[Title Page](#)[Abstract](#)[Introduction](#)[Conclusions](#)[References](#)[Tables](#)[Figures](#)[I◀](#)[▶I](#)[◀](#)[▶](#)[Back](#)[Close](#)[Full Screen / Esc](#)[Print Version](#)[Interactive Discussion](#)

Mesoscale modeling  
of combined aerosol  
and photo-oxidant  
processes

M. Lazaridis et al.

**Table 4.** Comparison between experimental field data and modelling results (gaseous species) for the July 2000 period at the research vessel Aigeaion.

Parameter	Aegean sea (summer) (ppbv)	Model Results (ppbv)
O <sub>3</sub>	59.4***	52.6
NO <sub>2</sub>	7.1***	3.5
SO <sub>2</sub>	1.56*	2.1
HNO <sub>3</sub>	0.33*	0.47
HONO	0.12**	0.05

\* from annular denuder measurements

\*\* prototype wet effluent diffusion denuder technique/chemiluniscent detection

\*\*\* prototype chemiluminescence ozone and nitrogen dioxide detectors

Title Page

Abstract

Introduction

Conclusions

References

Tables

Figures

◀

▶

◀

▶

Back

Close

Full Screen / Esc

Print Version

Interactive Discussion

Mesoscale modeling  
of combined aerosol  
and photo-oxidant  
processes

M. Lazaridis et al.

**Table 5.** Comparison between experimental field data and modelling results (gaseous species) for the January 2001 period at the Finokalia station.

Parameter	Finokalia (Winter) (ppbv)	Model Results (ppbv)
O <sub>3</sub>	41.7	31.3
NO <sub>2</sub>	0.52***	0.6
NO	<0.05	0.02
HNO <sub>3</sub>	0.04**	0.02
HONO	0.07**	0.03

\* from annular denuder measurements

\*\* prototype wet effluent diffusion denuder technique/chemiluniscent detection

\*\*\* prototype chemiluminescence ozone and nitrogen dioxide detectors

Title Page

Abstract

Introduction

Conclusions

References

Tables

Figures

◀

▶

◀

▶

Back

Close

Full Screen / Esc

Print Version

Interactive Discussion

## Mesoscale modeling of combined aerosol and photo-oxidant processes

M. Lazaridis et al.

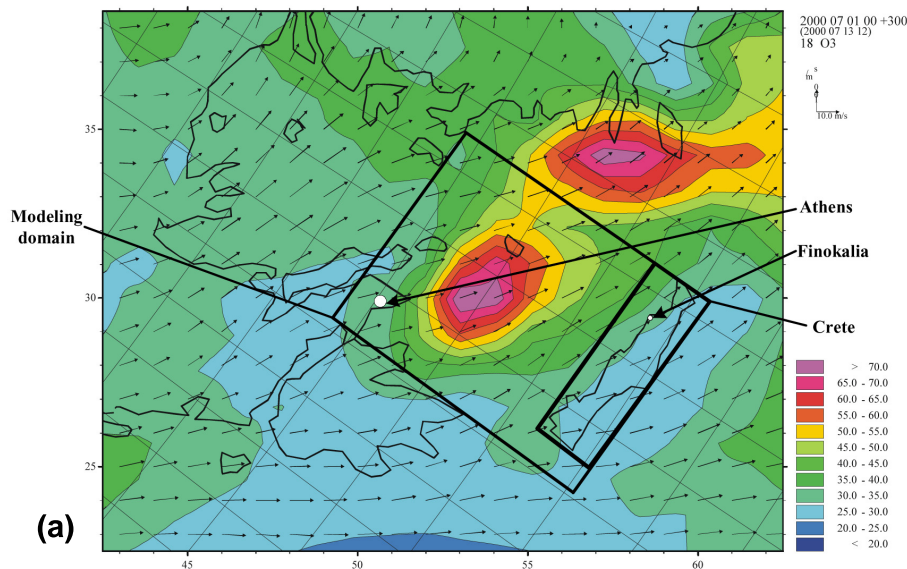


**Fig. 1.** Simulation results of the (a) ozone and (b) nitrogen oxides surface concentration for an extended grid using the CTM-NILU regional model (unit in ppb) on 13 July 2000.

[Title Page](#)[Abstract](#)[Introduction](#)[Conclusions](#)[References](#)[Tables](#)[Figures](#)[◀](#)[▶](#)[◀](#)[▶](#)[Back](#)[Close](#)[Full Screen / Esc](#)[Print Version](#)[Interactive Discussion](#)

## Mesoscale modeling of combined aerosol and photo-oxidant processes

M. Lazaridis et al.

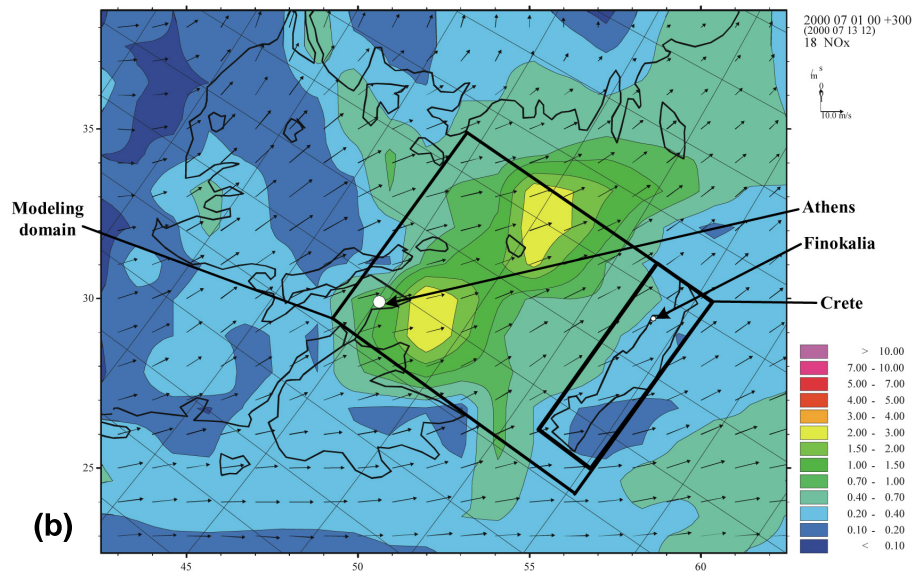


Fig. 1. Continued.

Title Page

Abstract

Introduction

Conclusions

References

Tables

Figures

◀

▶

◀

▶

Back

Close

Full Screen / Esc

Print Version

Interactive Discussion

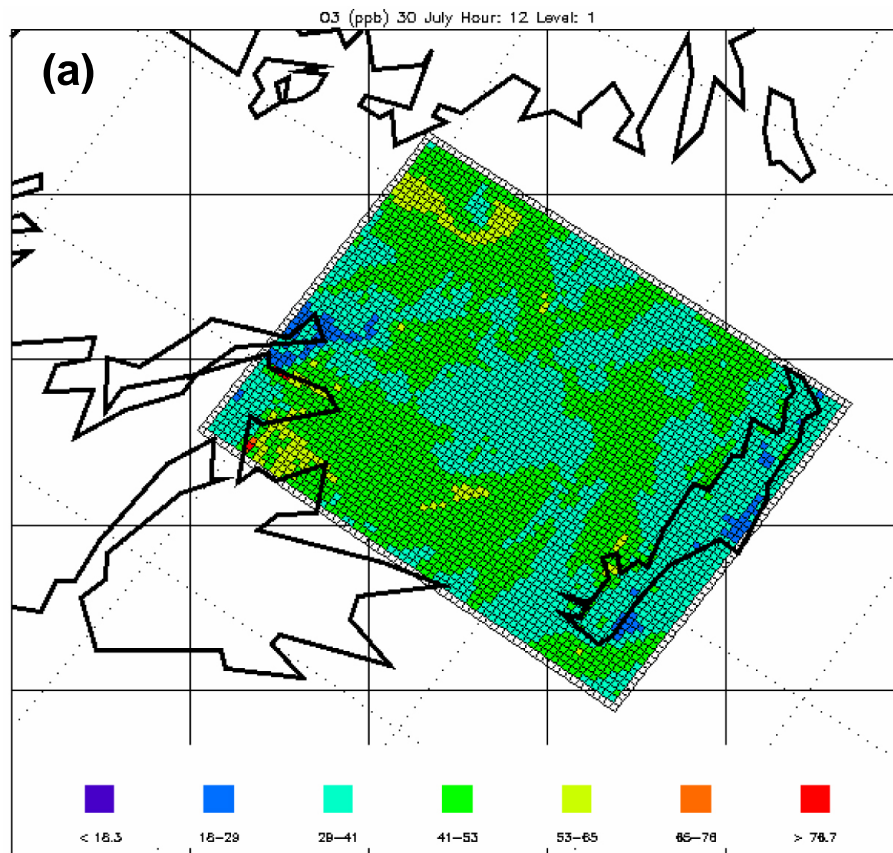


**Fig. 2.** Surface spatial distribution of (a) O<sub>3</sub> (b) NO<sub>2</sub> (c) SO<sub>2</sub> (d) Na<sup>+</sup> (e) NH<sub>4</sub><sup>+</sup> (f) CO, (g) resuspended dust and (h) PM<sub>10</sub> at 30 July 12:00 h.

**Mesoscale modeling  
of combined aerosol  
and photo-oxidant  
processes**

M. Lazaridis et al.

Title Page

Abstract

Introduction

Conclusions

References

Tables

Figures

◀

▶

◀

▶

Back

Close

Full Screen / Esc

Print Version

Interactive Discussion



**Mesoscale modeling  
of combined aerosol  
and photo-oxidant  
processes**

M. Lazaridis et al.

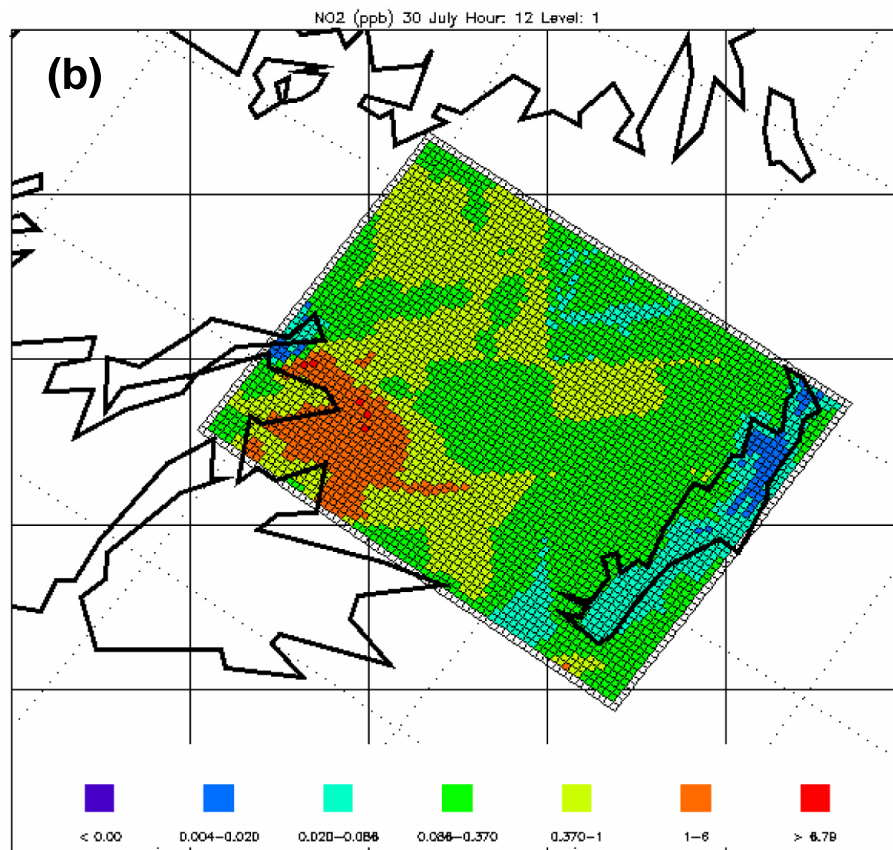


Fig. 2. Continued.

Title Page

Abstract

Introduction

Conclusions

References

Tables

Figures

I◀

▶I

◀

▶

Back

Close

Full Screen / Esc

Print Version

Interactive Discussion

**Mesoscale modeling  
of combined aerosol  
and photo-oxidant  
processes**

M. Lazaridis et al.

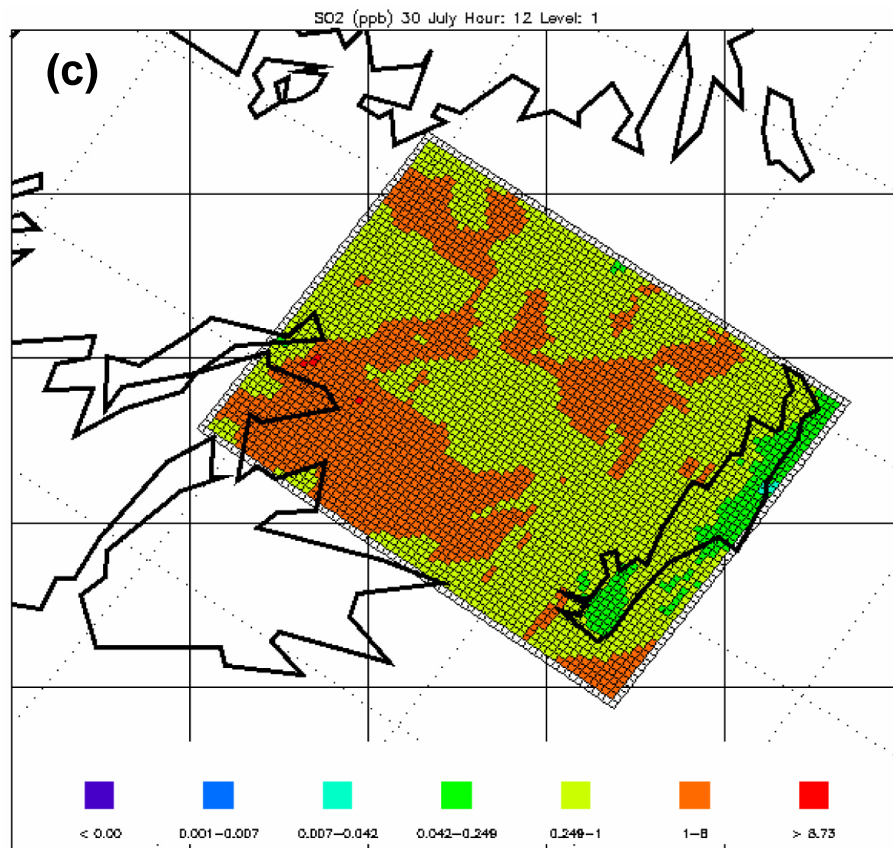
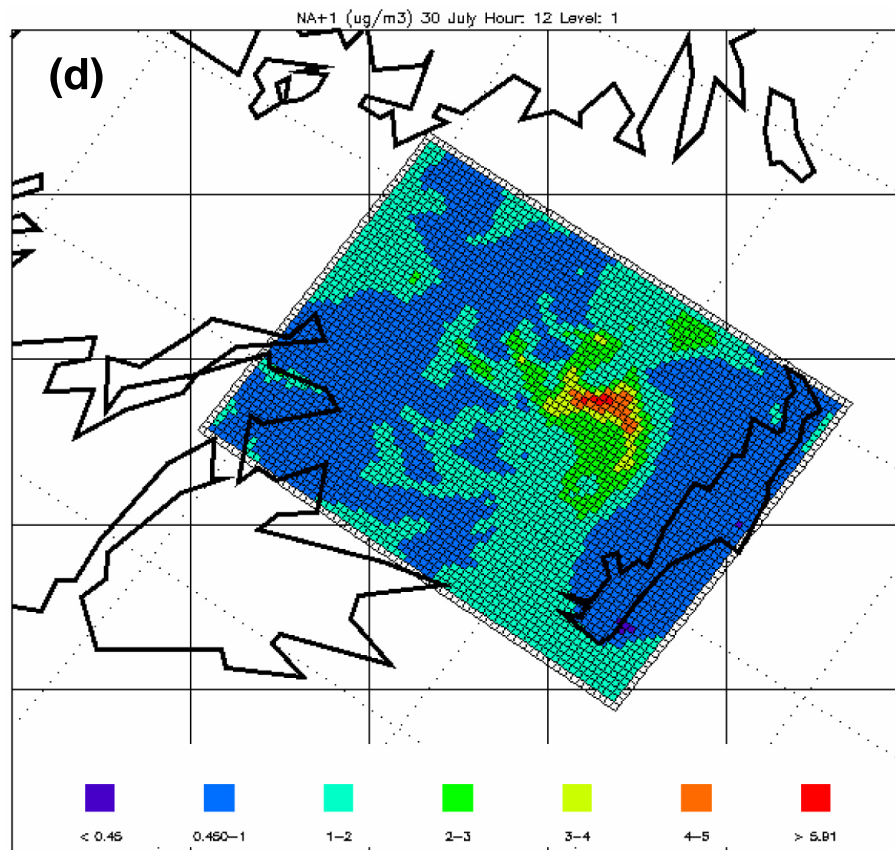


Fig. 2. Continued.

[Title Page](#)[Abstract](#)[Introduction](#)[Conclusions](#)[References](#)[Tables](#)[Figures](#)[I◀](#)[▶I](#)[◀](#)[▶](#)[Back](#)[Close](#)[Full Screen / Esc](#)[Print Version](#)[Interactive Discussion](#)

**Mesoscale modeling  
of combined aerosol  
and photo-oxidant  
processes**

M. Lazaridis et al.

**Fig. 2.** Continued.[Title Page](#)[Abstract](#)[Introduction](#)[Conclusions](#)[References](#)[Tables](#)[Figures](#)[◀](#)[▶](#)[◀](#)[▶](#)[Back](#)[Close](#)[Full Screen / Esc](#)[Print Version](#)[Interactive Discussion](#)

**Mesoscale modeling  
of combined aerosol  
and photo-oxidant  
processes**

M. Lazaridis et al.

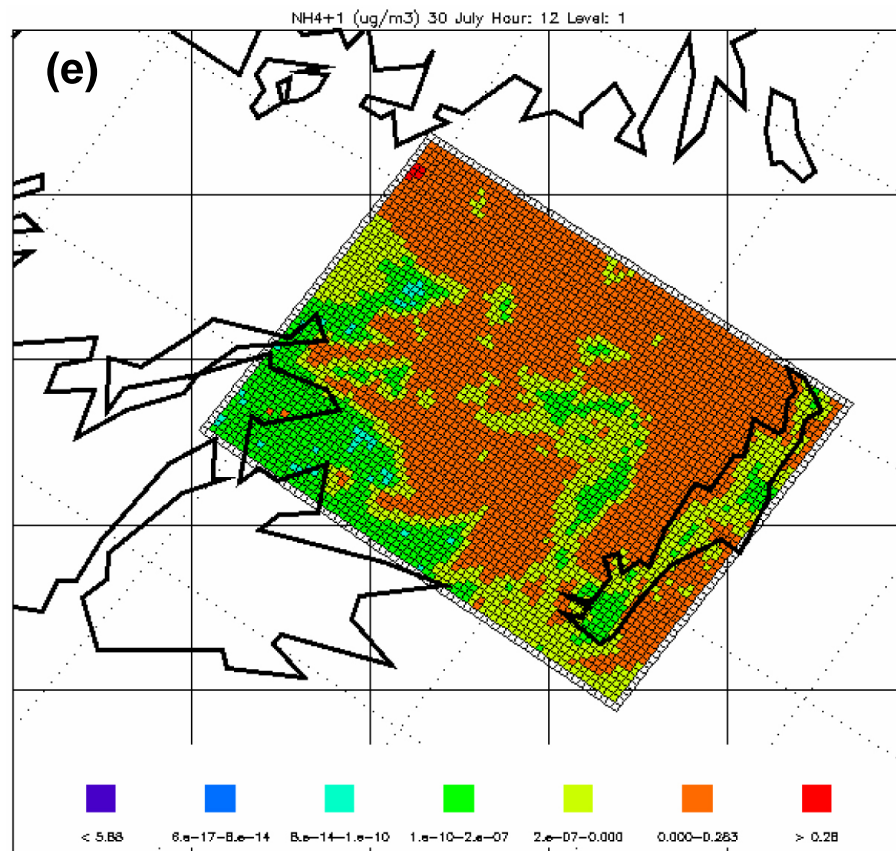


Fig. 2. Continued.

Title Page

Abstract

Introduction

Conclusions

References

Tables

Figures

◀

▶

◀

▶

Back

Close

Full Screen / Esc

Print Version

Interactive Discussion

**Mesoscale modeling  
of combined aerosol  
and photo-oxidant  
processes**

M. Lazaridis et al.

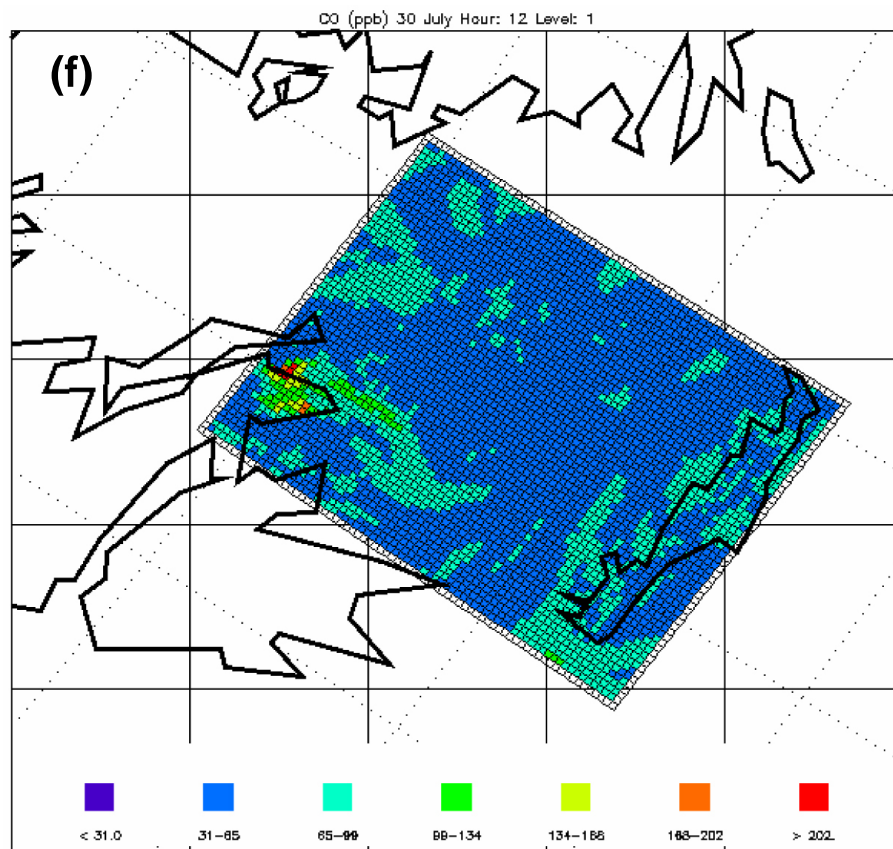


Fig. 2. Continued.

Title Page

Abstract

Introduction

Conclusions

References

Tables

Figures

◀

▶

◀

▶

Back

Close

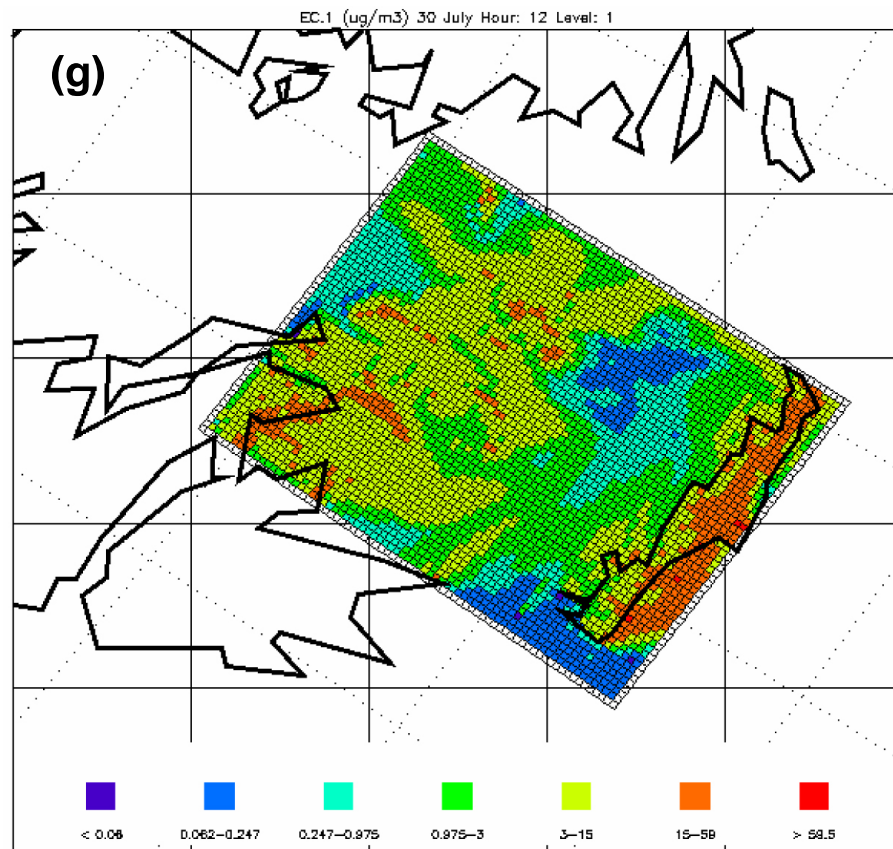
Full Screen / Esc

Print Version

Interactive Discussion

**Mesoscale modeling  
of combined aerosol  
and photo-oxidant  
processes**

M. Lazaridis et al.

**Fig. 2.** Continued.[Title Page](#)[Abstract](#)[Introduction](#)[Conclusions](#)[References](#)[Tables](#)[Figures](#)[I◀](#)[▶I](#)[◀](#)[▶](#)[Back](#)[Close](#)[Full Screen / Esc](#)[Print Version](#)[Interactive Discussion](#)



**Mesoscale modeling  
of combined aerosol  
and photo-oxidant  
processes**

M. Lazaridis et al.

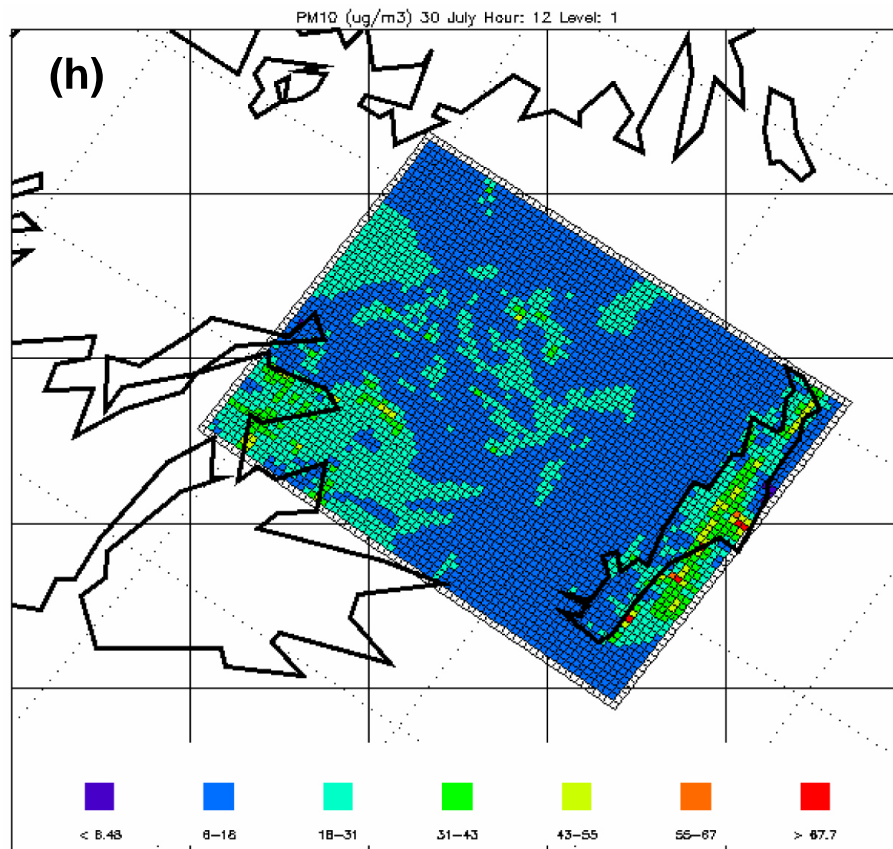


Fig. 2. Continued.

Title Page

Abstract

Introduction

Conclusions

References

Tables

Figures

I◀

▶I

◀

▶

Back

Close

Full Screen / Esc

Print Version

Interactive Discussion

**Mesoscale modeling  
of combined aerosol  
and photo-oxidant  
processes**

M. Lazaridis et al.

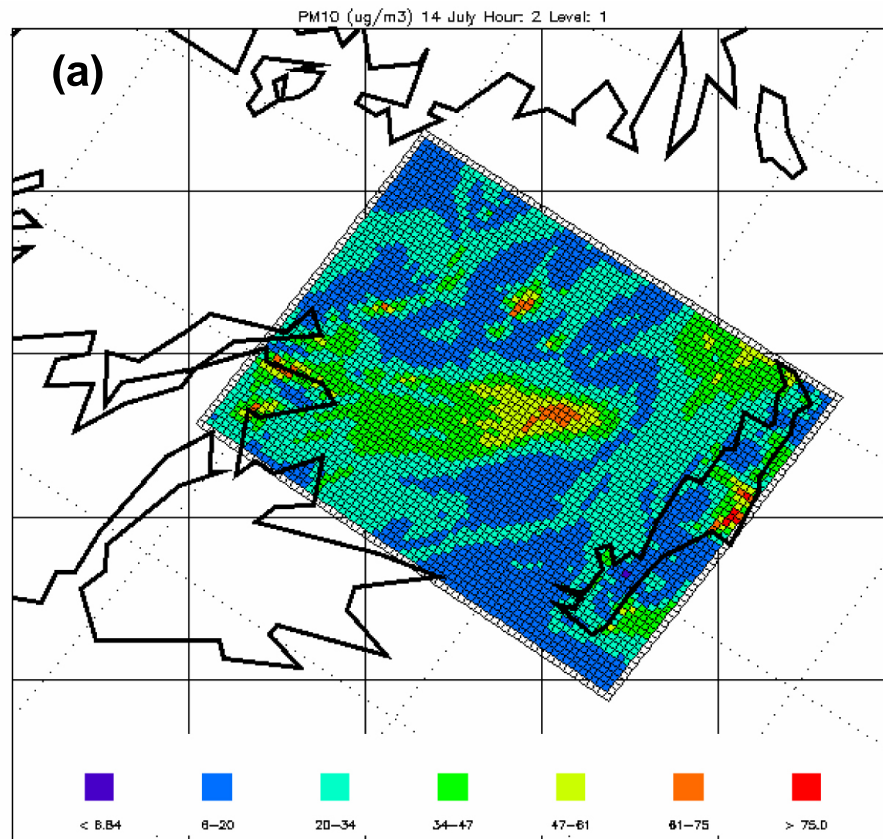


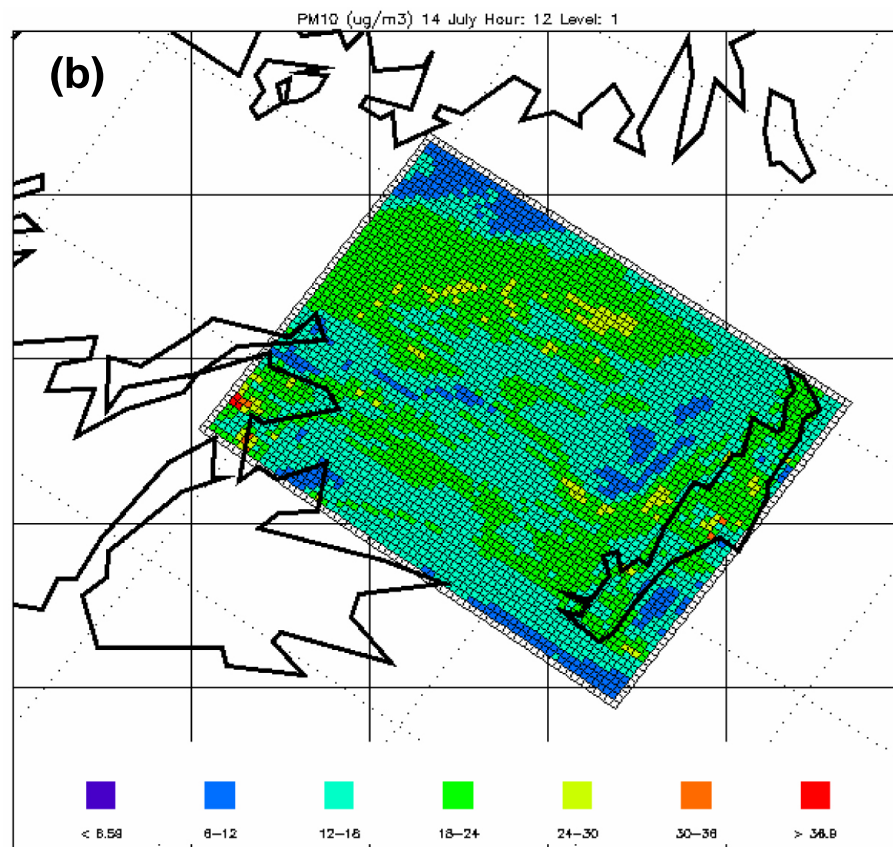
**Fig. 3.** Surface spatial distribution of  $\text{PM}_{10}$  at 14 July at (a) 02:00 h, (b) 12:00 h, (c) 14:00 h, (d) 16:00 h, (e) 17:00 h, (f) 21:00 h and (g) 24:00 h.

[Title Page](#)[Abstract](#)[Introduction](#)[Conclusions](#)[References](#)[Tables](#)[Figures](#)[I◀](#)[▶I](#)[◀](#)[▶](#)[Back](#)[Close](#)[Full Screen / Esc](#)[Print Version](#)[Interactive Discussion](#)



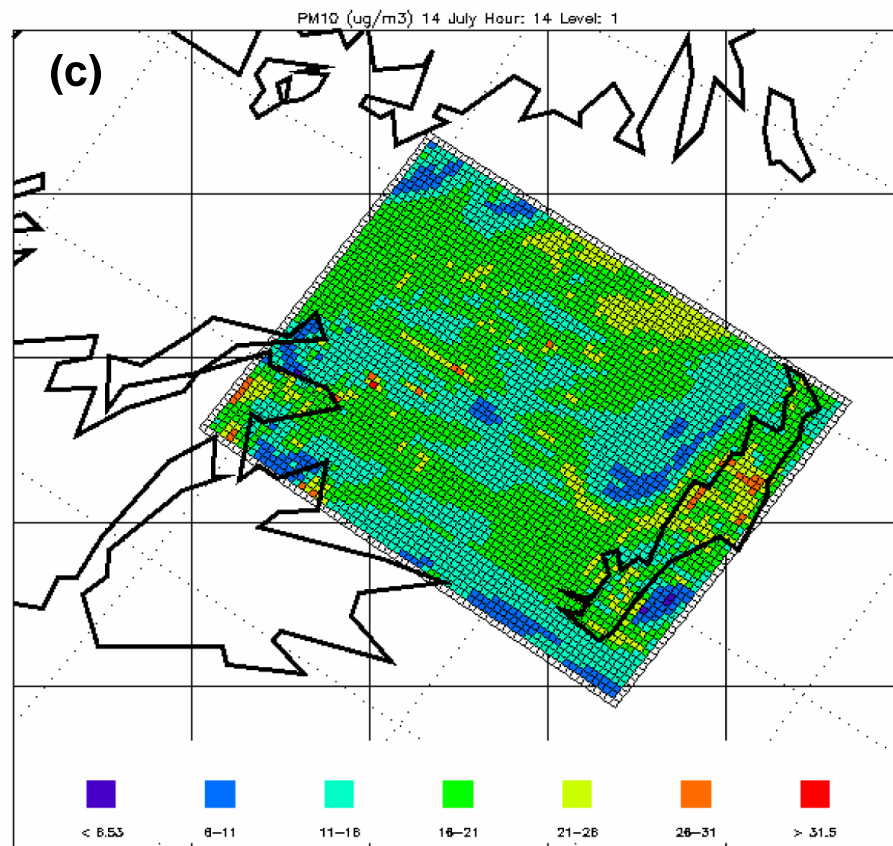
**Mesoscale modeling  
of combined aerosol  
and photo-oxidant  
processes**

M. Lazaridis et al.

**Fig. 3.** Continued.[Title Page](#)[Abstract](#)[Introduction](#)[Conclusions](#)[References](#)[Tables](#)[Figures](#)[I◀](#)[▶I](#)[◀](#)[▶](#)[Back](#)[Close](#)[Full Screen / Esc](#)[Print Version](#)[Interactive Discussion](#)

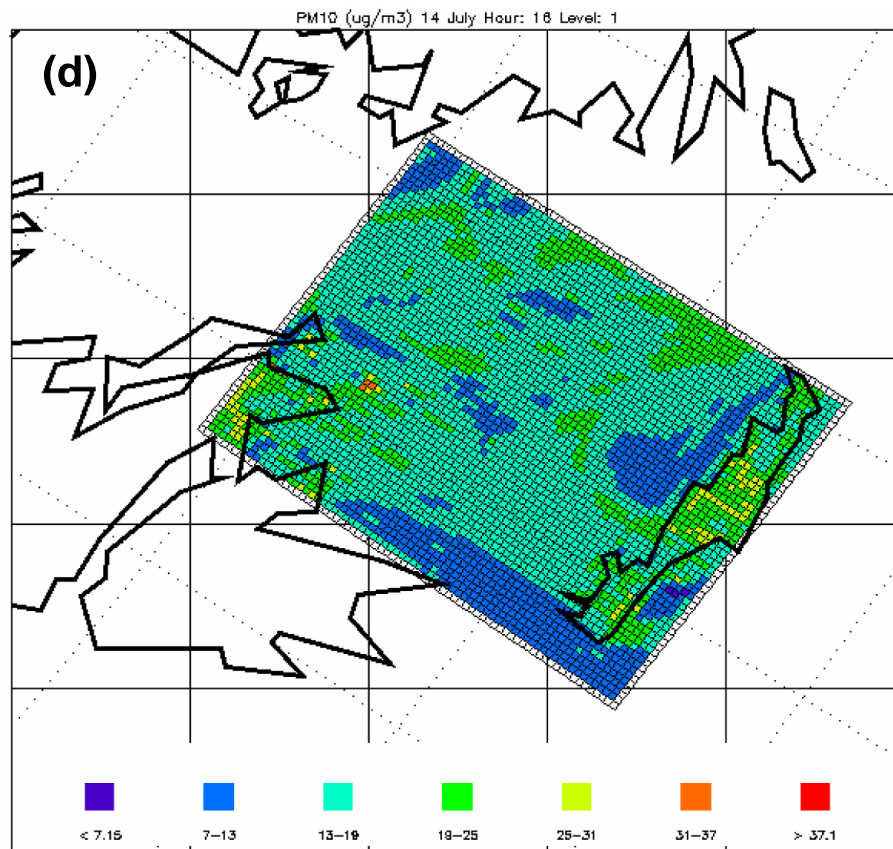
**Mesoscale modeling  
of combined aerosol  
and photo-oxidant  
processes**

M. Lazaridis et al.

**Fig. 3.** Continued.[Title Page](#)[Abstract](#)[Introduction](#)[Conclusions](#)[References](#)[Tables](#)[Figures](#)[I◀](#)[▶I](#)[◀](#)[▶](#)[Back](#)[Close](#)[Full Screen / Esc](#)[Print Version](#)[Interactive Discussion](#)

**Mesoscale modeling  
of combined aerosol  
and photo-oxidant  
processes**

M. Lazaridis et al.

**Fig. 3.** Continued.[Title Page](#)[Abstract](#)[Introduction](#)[Conclusions](#)[References](#)[Tables](#)[Figures](#)[I◀](#)[▶I](#)[◀](#)[▶](#)[Back](#)[Close](#)[Full Screen / Esc](#)[Print Version](#)[Interactive Discussion](#)

**Mesoscale modeling  
of combined aerosol  
and photo-oxidant  
processes**

M. Lazaridis et al.

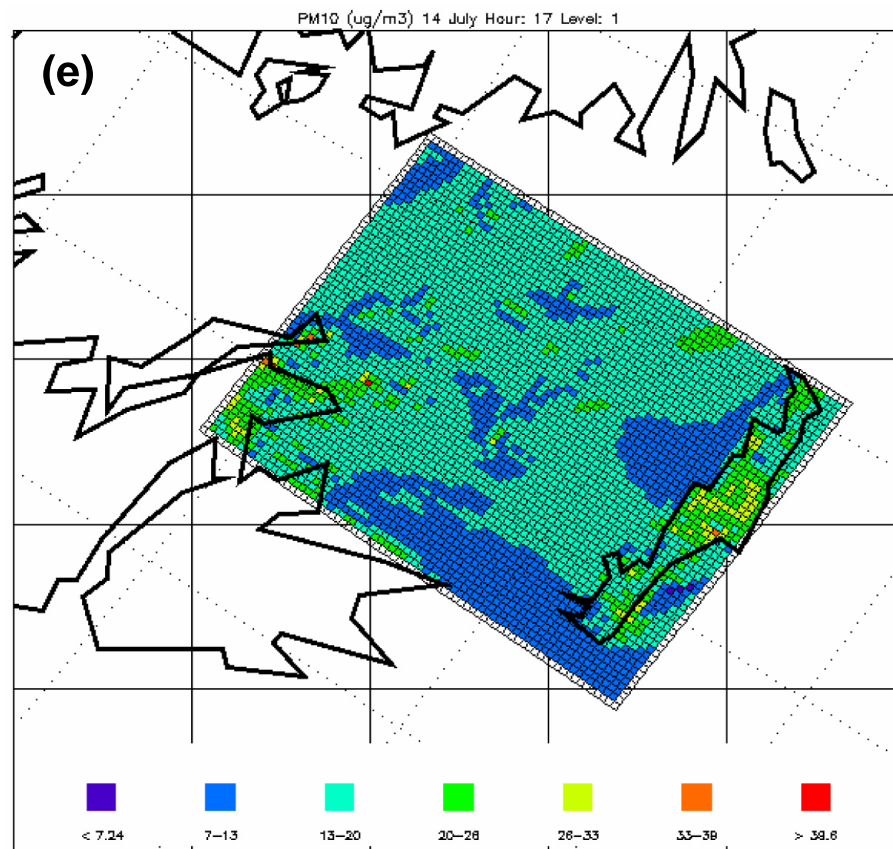


Fig. 3. Continued.

Title Page

Abstract

Introduction

Conclusions

References

Tables

Figures

I◀

▶I

◀

▶

Back

Close

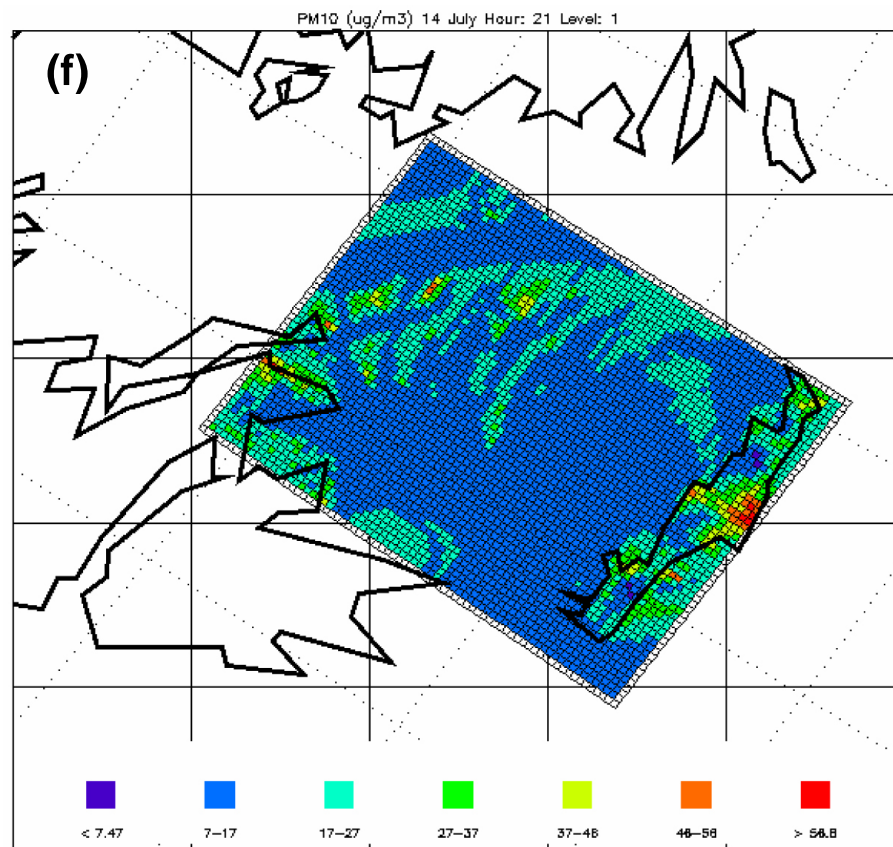
Full Screen / Esc

Print Version

Interactive Discussion

**Mesoscale modeling  
of combined aerosol  
and photo-oxidant  
processes**

M. Lazaridis et al.

**Fig. 3.** Continued.

Title Page

Abstract

Introduction

Conclusions

References

Tables

Figures

I◀

▶I

◀

▶

Back

Close

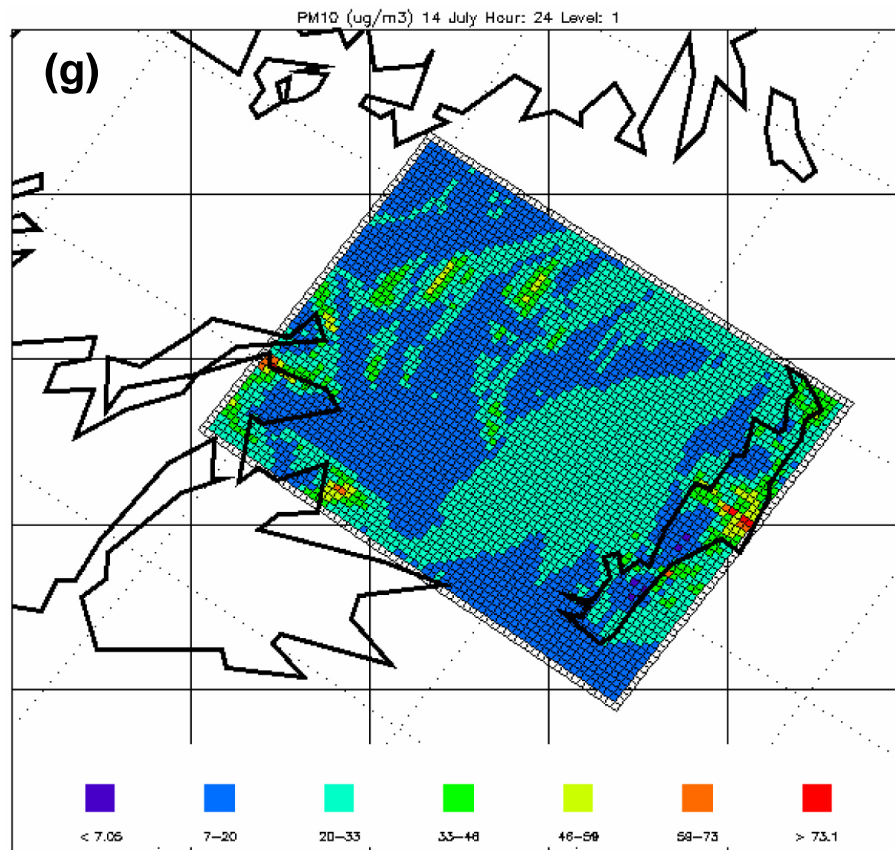
Full Screen / Esc

Print Version

Interactive Discussion

**Mesoscale modeling  
of combined aerosol  
and photo-oxidant  
processes**

M. Lazaridis et al.

**Fig. 3.** Continued.[Title Page](#)[Abstract](#)[Introduction](#)[Conclusions](#)[References](#)[Tables](#)[Figures](#)[I◀](#)[▶I](#)[◀](#)[▶](#)[Back](#)[Close](#)[Full Screen / Esc](#)[Print Version](#)[Interactive Discussion](#)



**Mesoscale modeling  
of combined aerosol  
and photo-oxidant  
processes**

M. Lazaridis et al.

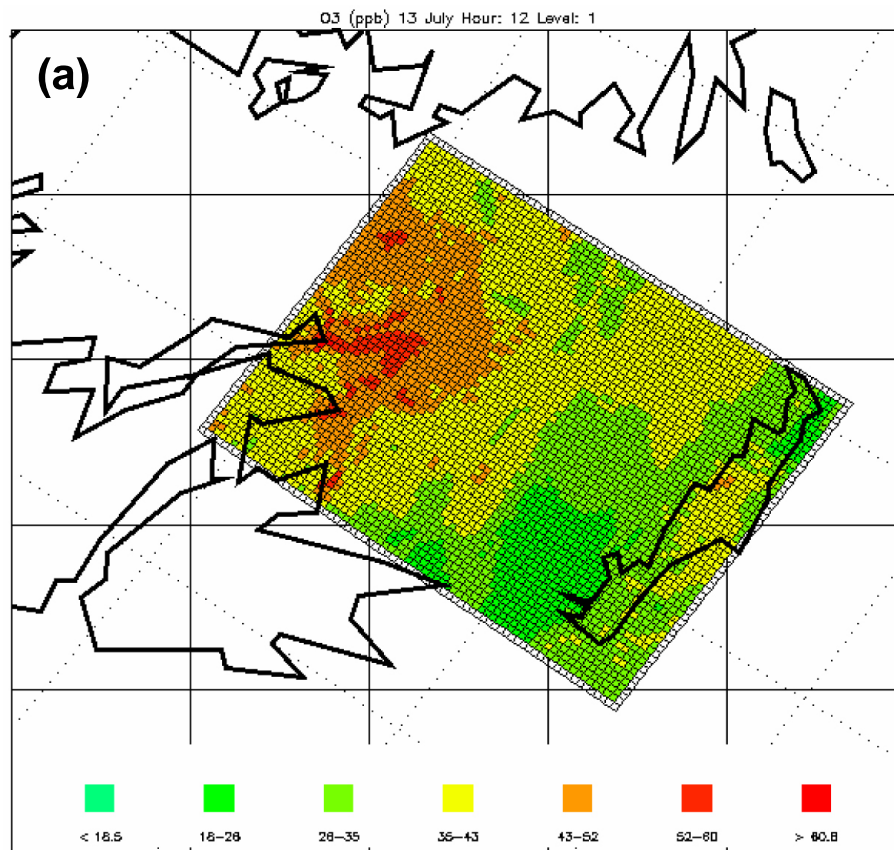


**Fig. 4.** Surface spatial distribution of O<sub>3</sub> and PM<sub>10</sub> for 13 July 2000 (a–b), 14 July 2000 (c–d), 15 July 2000 (e–f) and 16 July 2000 (g–h).

[Title Page](#)[Abstract](#)[Introduction](#)[Conclusions](#)[References](#)[Tables](#)[Figures](#)[◀](#)[▶](#)[◀](#)[▶](#)[Back](#)[Close](#)[Full Screen / Esc](#)[Print Version](#)[Interactive Discussion](#)

**Mesoscale modeling  
of combined aerosol  
and photo-oxidant  
processes**

M. Lazaridis et al.

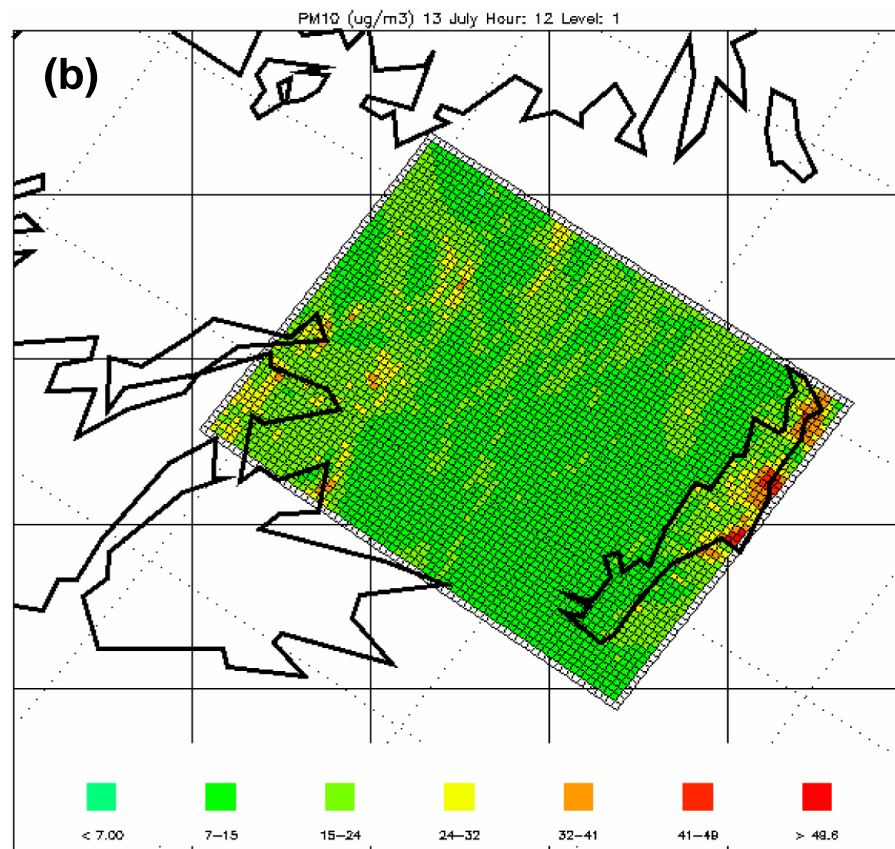


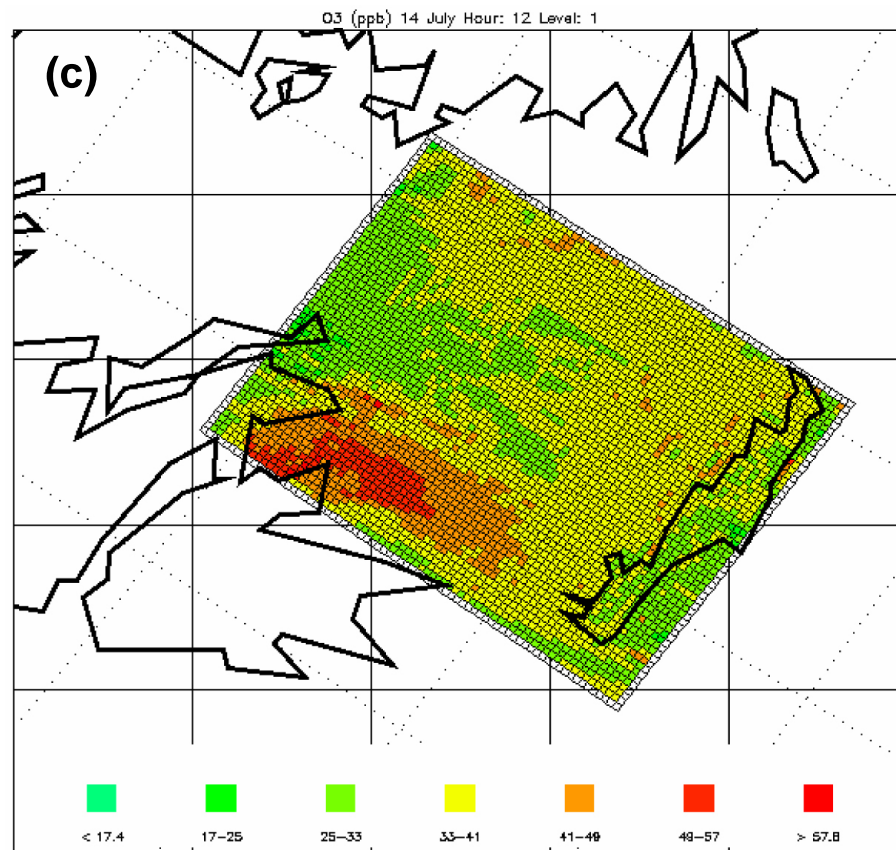
Fig. 4. Continued.

[Title Page](#)[Abstract](#)[Introduction](#)[Conclusions](#)[References](#)[Tables](#)[Figures](#)[I◀](#)[▶I](#)[◀](#)[▶](#)[Back](#)[Close](#)[Full Screen / Esc](#)[Print Version](#)[Interactive Discussion](#)



**Mesoscale modeling  
of combined aerosol  
and photo-oxidant  
processes**

M. Lazaridis et al.

**Fig. 4.** Continued.[Title Page](#)[Abstract](#)[Introduction](#)[Conclusions](#)[References](#)[Tables](#)[Figures](#)[I◀](#)[▶I](#)[◀](#)[▶](#)[Back](#)[Close](#)[Full Screen / Esc](#)[Print Version](#)[Interactive Discussion](#)

**Mesoscale modeling  
of combined aerosol  
and photo-oxidant  
processes**

M. Lazaridis et al.

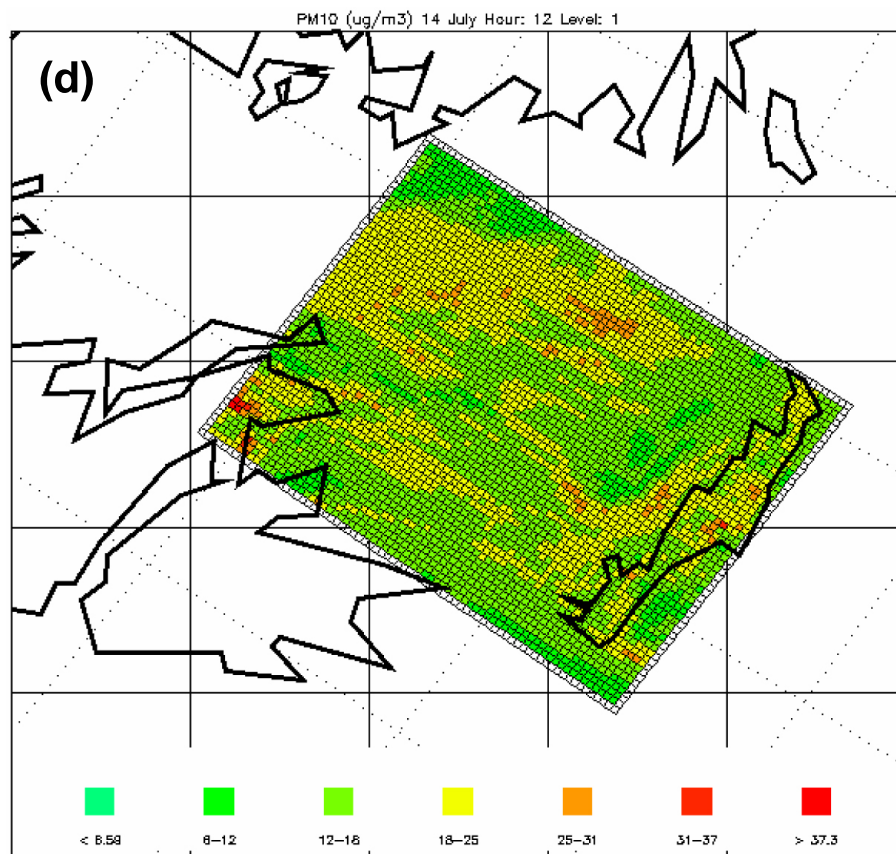


Fig. 4. Continued.

[Title Page](#)[Abstract](#)[Introduction](#)[Conclusions](#)[References](#)[Tables](#)[Figures](#)[I◀](#)[▶I](#)[◀](#)[▶](#)[Back](#)[Close](#)[Full Screen / Esc](#)[Print Version](#)[Interactive Discussion](#)

**Mesoscale modeling  
of combined aerosol  
and photo-oxidant  
processes**

M. Lazaridis et al.

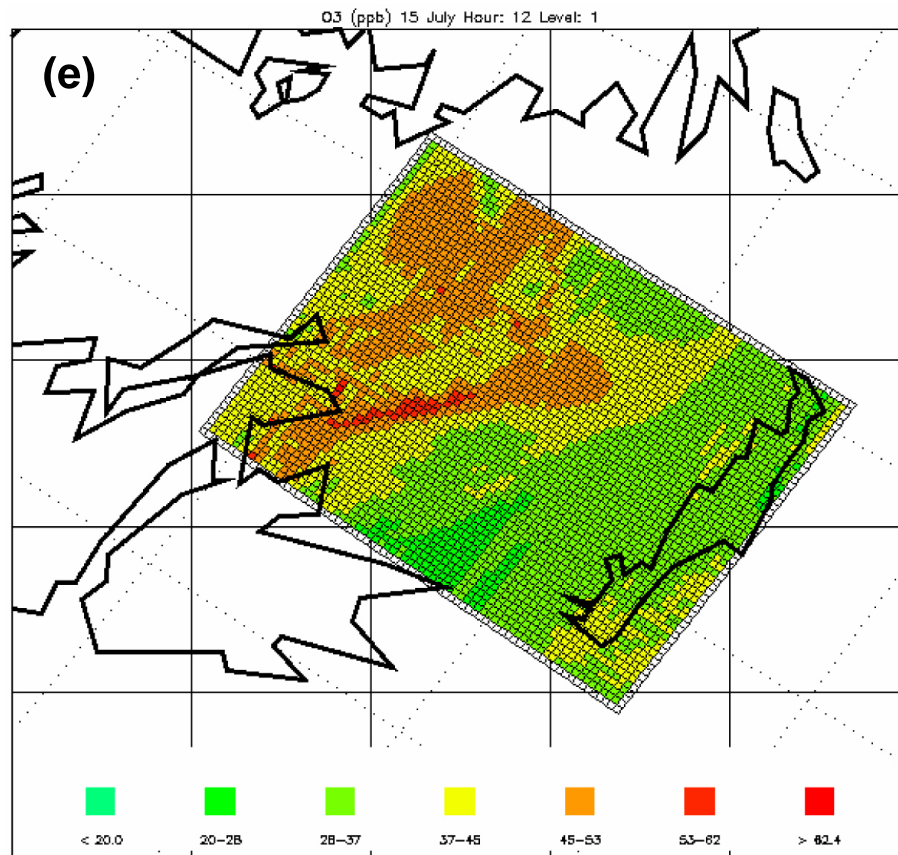
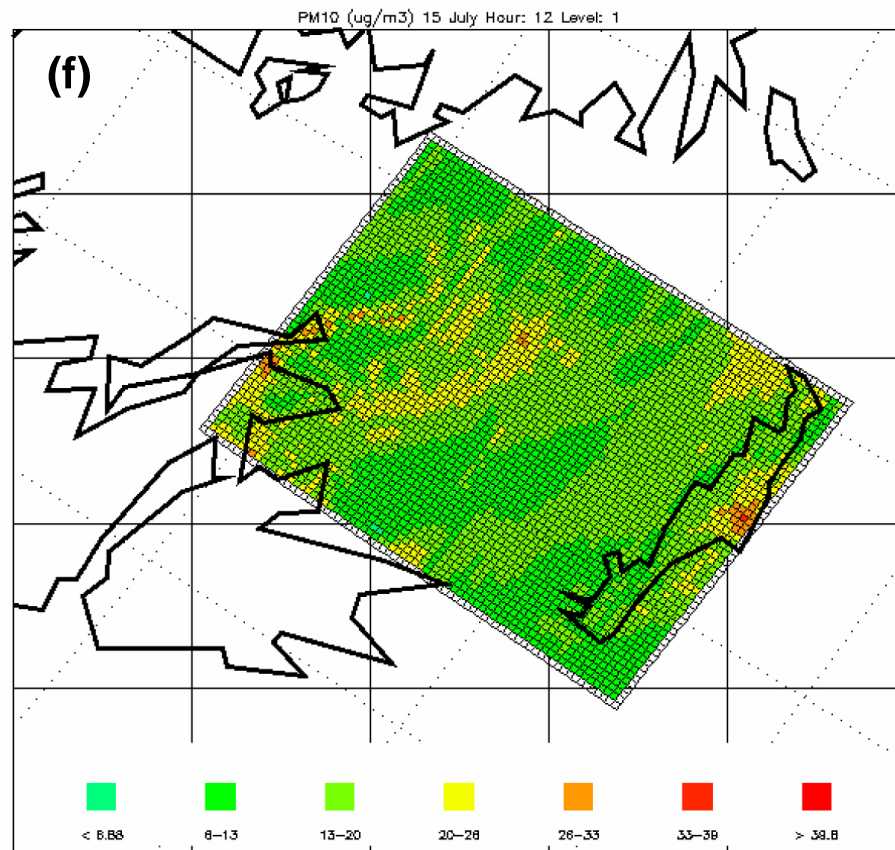


Fig. 4. Continued.

[Title Page](#)[Abstract](#)[Introduction](#)[Conclusions](#)[References](#)[Tables](#)[Figures](#)[I◀](#)[▶I](#)[◀](#)[▶](#)[Back](#)[Close](#)[Full Screen / Esc](#)[Print Version](#)[Interactive Discussion](#)

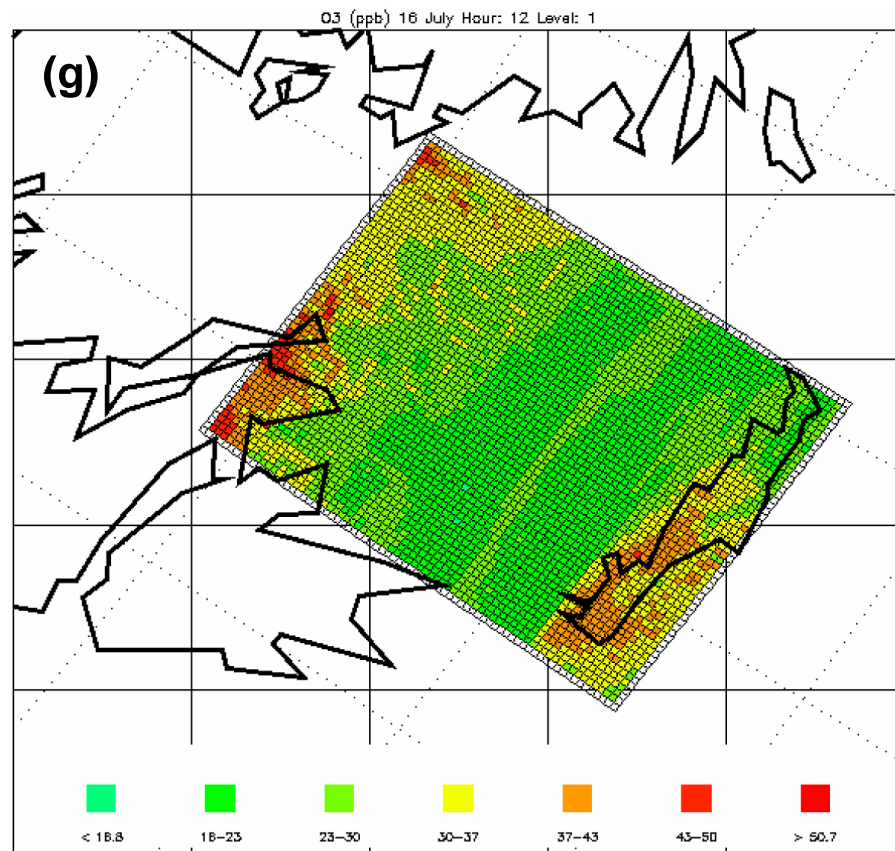
**Mesoscale modeling  
of combined aerosol  
and photo-oxidant  
processes**

M. Lazaridis et al.

**Fig. 4.** Continued.[Title Page](#)[Abstract](#)[Introduction](#)[Conclusions](#)[References](#)[Tables](#)[Figures](#)[◀](#)[▶](#)[◀](#)[▶](#)[Back](#)[Close](#)[Full Screen / Esc](#)[Print Version](#)[Interactive Discussion](#)

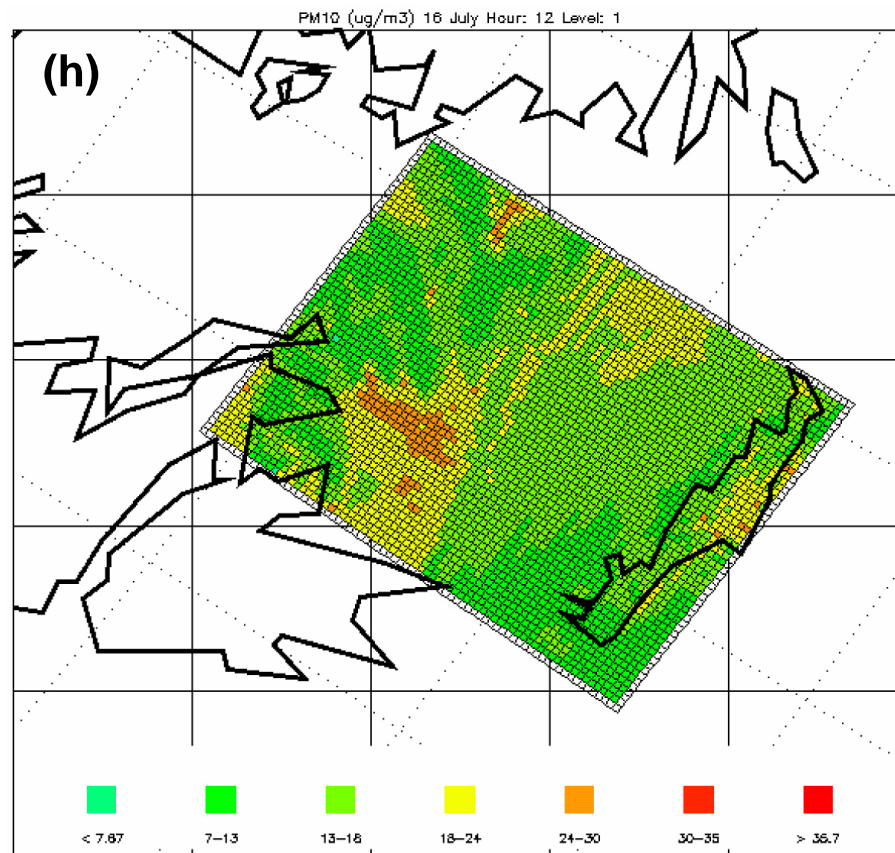
**Mesoscale modeling  
of combined aerosol  
and photo-oxidant  
processes**

M. Lazaridis et al.

**Fig. 4.** Continued.[Title Page](#)[Abstract](#)[Introduction](#)[Conclusions](#)[References](#)[Tables](#)[Figures](#)[◀](#)[▶](#)[◀](#)[▶](#)[Back](#)[Close](#)[Full Screen / Esc](#)[Print Version](#)[Interactive Discussion](#)

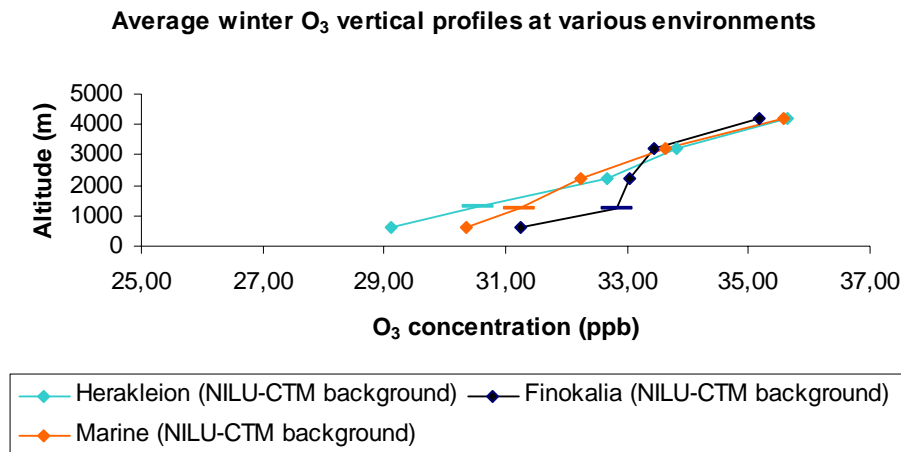
**Mesoscale modeling  
of combined aerosol  
and photo-oxidant  
processes**

M. Lazaridis et al.

**Fig. 4.** Continued.[Title Page](#)[Abstract](#)[Introduction](#)[Conclusions](#)[References](#)[Tables](#)[Figures](#)[I◀](#)[▶I](#)[◀](#)[▶](#)[Back](#)[Close](#)[Full Screen / Esc](#)[Print Version](#)[Interactive Discussion](#)

**Mesoscale modeling  
of combined aerosol  
and photo-oxidant  
processes**

M. Lazaridis et al.

**Fig. 5.** Average vertical profile of ozone during January 2000 for three different environments.[Title Page](#)[Abstract](#)[Introduction](#)[Conclusions](#)[References](#)[Tables](#)[Figures](#)[◀](#)[▶](#)[◀](#)[▶](#)[Back](#)[Close](#)[Full Screen / Esc](#)[Print Version](#)[Interactive Discussion](#)

**Mesoscale modeling  
of combined aerosol  
and photo-oxidant  
processes**

M. Lazaridis et al.

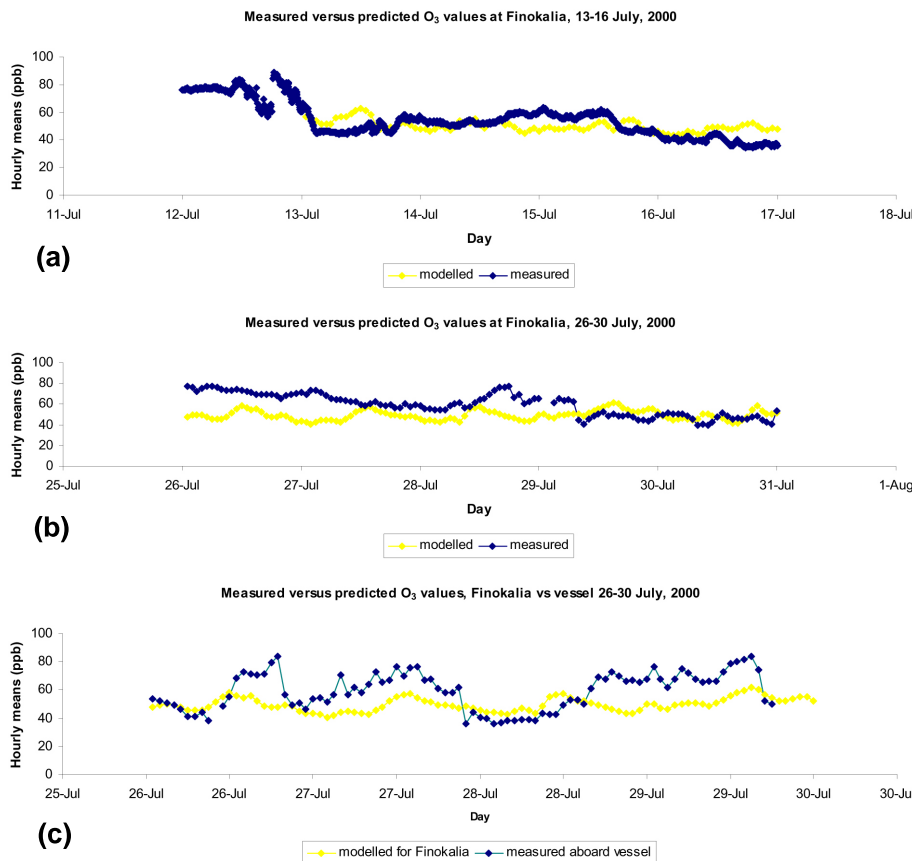


**Fig. 6.** Comparison between modeled and measured ozone concentrations for the period **(a)** 13–16 July 2000 at Finokalia, **(b)** 26–30 July 2000 at Finokalia, **(c)** 26–30 July 2000 onboard the research vessel Aigeaion, **(d)** 7–15 January 2001 at Finokalia, **(e)** 7–15 January 2001 at Herakleion.

Title Page

Abstract

Introduction

Conclusions

References

Tables

Figures

◀

▶

◀

▶

Back

Close

Full Screen / Esc

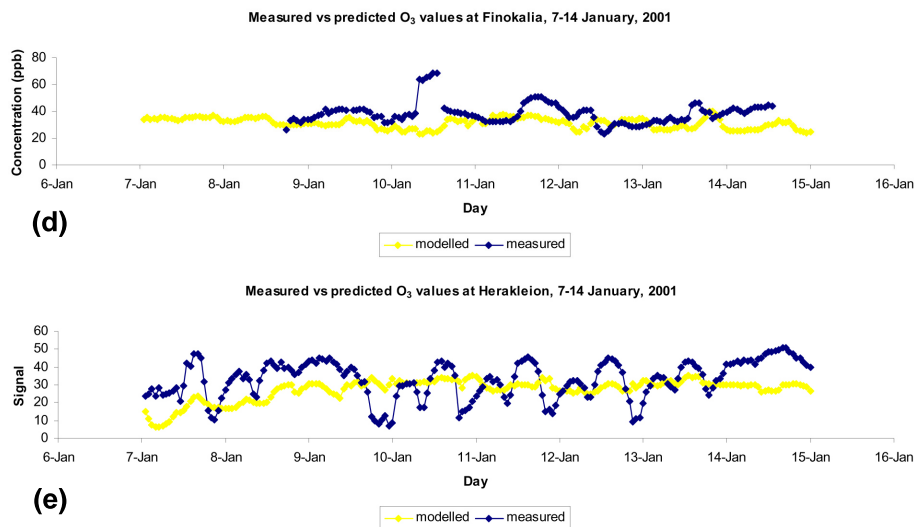
Print Version

Interactive Discussion



**Mesoscale modeling  
of combined aerosol  
and photo-oxidant  
processes**

M. Lazaridis et al.

**Fig. 6.** Continued.

Title Page

Abstract

Introduction

Conclusions

References

Tables

Figures

◀

▶

◀

▶

Back

Close

Full Screen / Esc

Print Version

Interactive Discussion

**Mesoscale modeling  
of combined aerosol  
and photo-oxidant  
processes**

M. Lazaridis et al.

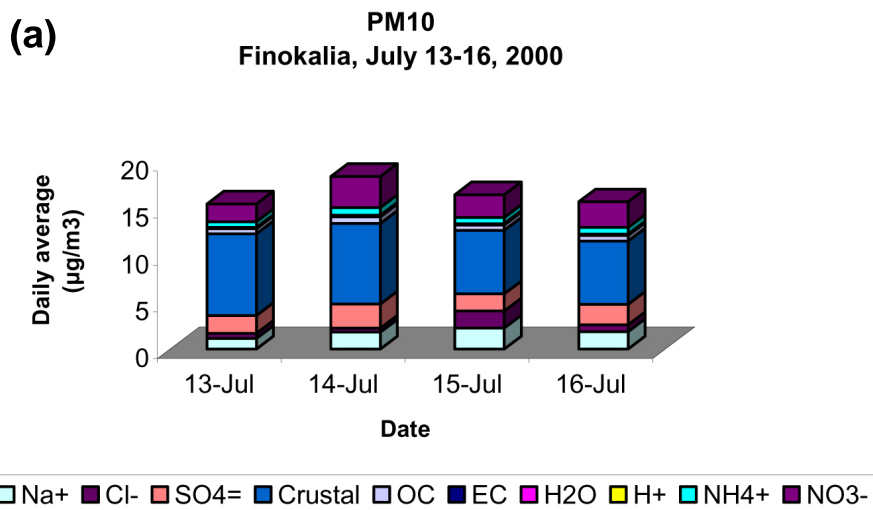


**Fig. 7.** Chemical resolved PM<sub>10</sub> mass between (a) 13–16 July 2000, (b) 26–30 July 2000, (c) 7–14 January 2001.

[Title Page](#)[Abstract](#)[Introduction](#)[Conclusions](#)[References](#)[Tables](#)[Figures](#)[◀](#)[▶](#)[◀](#)[▶](#)[Back](#)[Close](#)[Full Screen / Esc](#)[Print Version](#)[Interactive Discussion](#)

**Mesoscale modeling  
of combined aerosol  
and photo-oxidant  
processes**

M. Lazaridis et al.

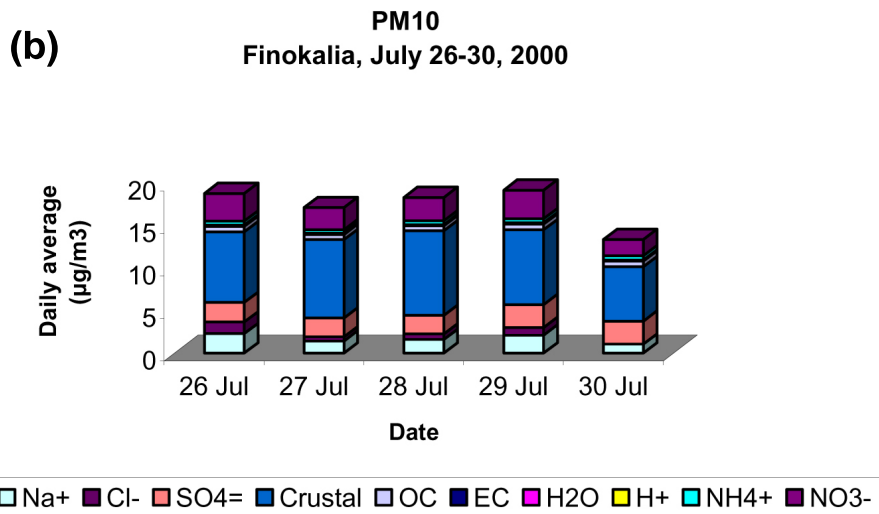


Fig. 7. Continued.

Title Page

Abstract

Introduction

Conclusions

References

Tables

Figures

◀

▶

◀

▶

Back

Close

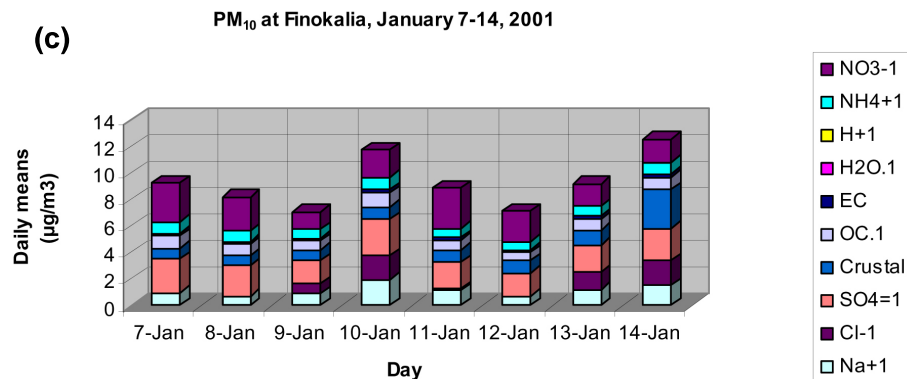
Full Screen / Esc

Print Version

Interactive Discussion

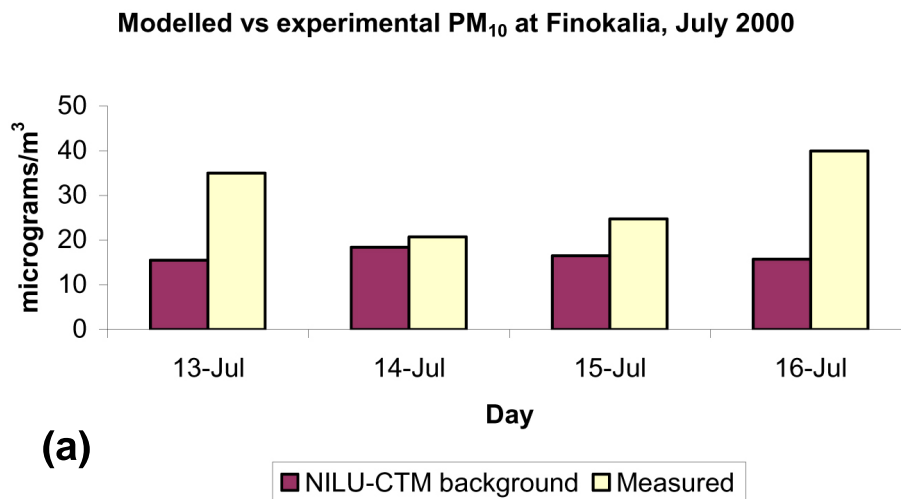
**Mesoscale modeling  
of combined aerosol  
and photo-oxidant  
processes**

M. Lazaridis et al.

**Fig. 7.** Continued.[Title Page](#)[Abstract](#)[Introduction](#)[Conclusions](#)[References](#)[Tables](#)[Figures](#)[I◀](#)[▶I](#)[◀](#)[▶](#)[Back](#)[Close](#)[Full Screen / Esc](#)[Print Version](#)[Interactive Discussion](#)

**Mesoscale modeling  
of combined aerosol  
and photo-oxidant  
processes**

M. Lazaridis et al.

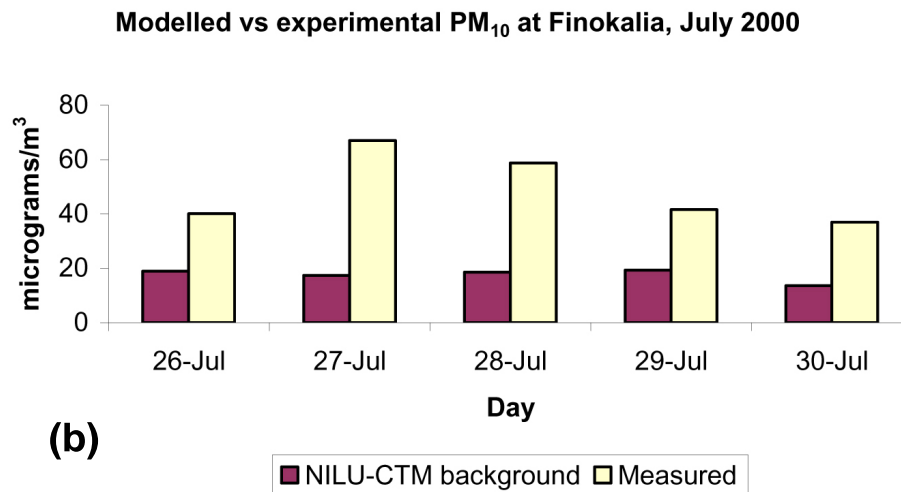


**Fig. 8.** Comparison between modelling and observed PM<sub>10</sub> mass concentration between (a) 13–16 July 2000, (b) 26–30 July 2000, (c) 7–13 January 2000 at the Finokalia station.

[Title Page](#)[Abstract](#)[Introduction](#)[Conclusions](#)[References](#)[Tables](#)[Figures](#)[◀](#)[▶](#)[◀](#)[▶](#)[Back](#)[Close](#)[Full Screen / Esc](#)[Print Version](#)[Interactive Discussion](#)

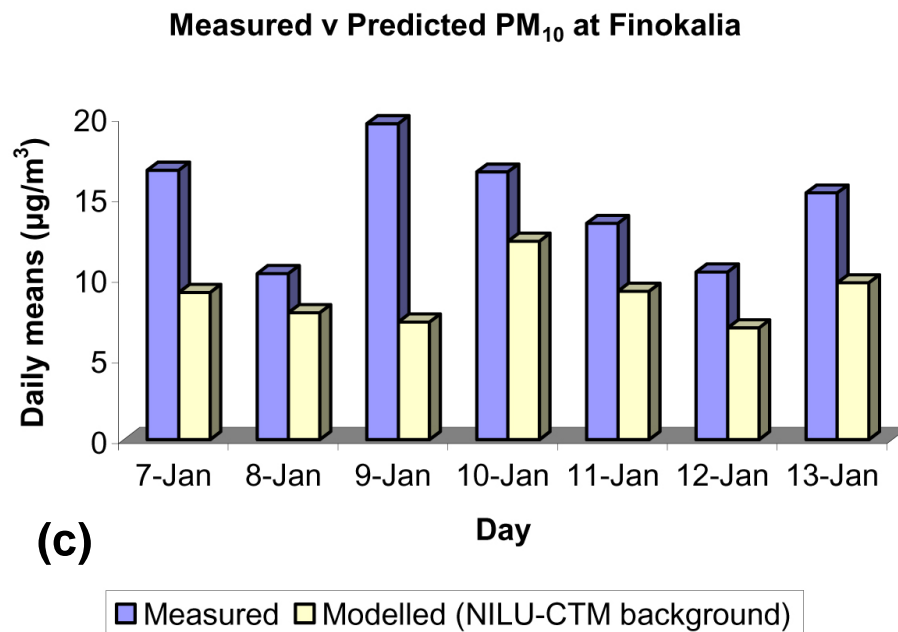
**Mesoscale modeling  
of combined aerosol  
and photo-oxidant  
processes**

M. Lazaridis et al.

**Fig. 8.** Continued.[Title Page](#)[Abstract](#)[Introduction](#)[Conclusions](#)[References](#)[Tables](#)[Figures](#)[◀](#)[▶](#)[◀](#)[▶](#)[Back](#)[Close](#)[Full Screen / Esc](#)[Print Version](#)[Interactive Discussion](#)

**Mesoscale modeling  
of combined aerosol  
and photo-oxidant  
processes**

M. Lazaridis et al.

**Fig. 8.** Continued.[Title Page](#)[Abstract](#)[Introduction](#)[Conclusions](#)[References](#)[Tables](#)[Figures](#)[◀](#)[▶](#)[◀](#)[▶](#)[Back](#)[Close](#)[Full Screen / Esc](#)[Print Version](#)[Interactive Discussion](#)

**Mesoscale modeling  
of combined aerosol  
and photo-oxidant  
processes**

M. Lazaridis et al.

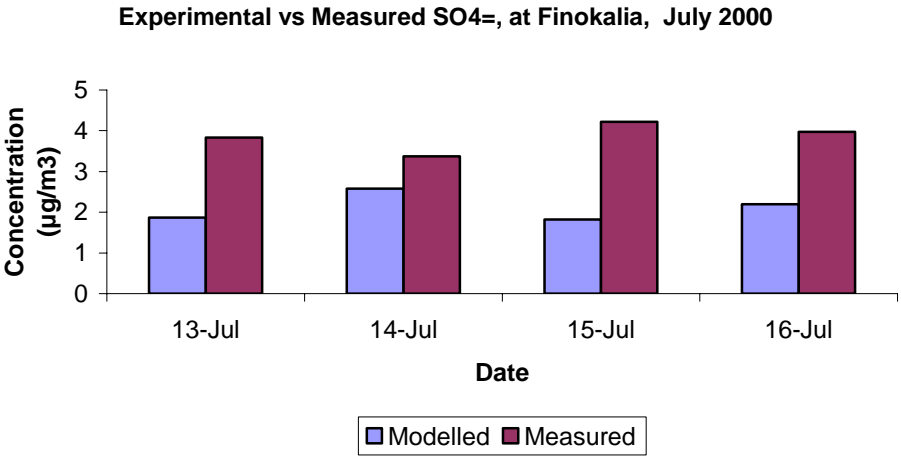


**Fig. 9.** Comparison between modelling and observed SO<sub>4</sub> mass concentration between 13–16 July 2000 at the Finokalia station.

Title Page

Abstract

Introduction

Conclusions

References

Tables

Figures

◀

▶

◀

▶

Back

Close

Full Screen / Esc

Print Version

Interactive Discussion



**Mesoscale modeling  
of combined aerosol  
and photo-oxidant  
processes**

M. Lazaridis et al.

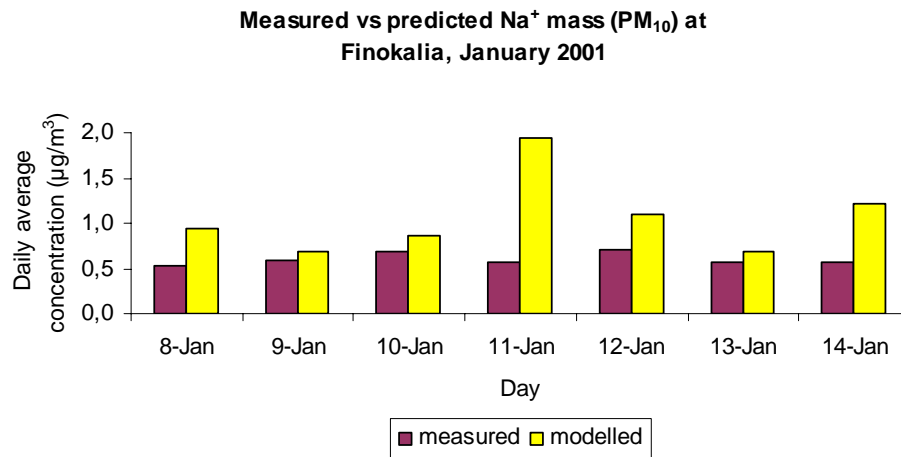


**Fig. 10.** Comparison between modelling and observed  $\text{Na}^+$  mass concentration between 8–14 January 2000 at the Finokalia station.

[Title Page](#)[Abstract](#)[Introduction](#)[Conclusions](#)[References](#)[Tables](#)[Figures](#)[◀](#)[▶](#)[◀](#)[▶](#)[Back](#)[Close](#)[Full Screen / Esc](#)[Print Version](#)[Interactive Discussion](#)